RESEARCH ARTICLE

RUNNING HEAD: NFAT5 osmoregulation of tilapia *myo*-inositol biosynthesis

Transcriptional up-regulation of the *myo*-Inositol biosynthesis pathway is enhanced by NFAT5 in hyper-osmotically stressed tilapia cells

Jens Hamar,[1] Avner Cnaani,[2] Dietmar Kültz[1]

[1]Department of Animal Sciences and Genome Center, University of California Davis, Davis, California, United States
[2] Department of Poultry and Aquaculture, Institute of Animal Sciences, Agricultural Research Organization, Rishon LeZion, Israel

Correspondence: *Dietmar Kültz (dkueltz@ucdavis.edu).*

ABSTRACT

Euryhaline fish experience variable osmotic environments requiring physiological adjustments to tolerate elevated salinity. Mozambique tilapia (*Oreochromis mossambicus*) possess one of the highest salinity tolerance limits of any fish. In tilapia and other euryhaline fish species the *myo*-inositol biosynthesis (MIB) pathway enzymes, *myo*-inositol phosphate synthase (MIPS) and inositol monophosphatase 1 (IMPA1.1), are among the most upregulated mRNAs and proteins indicating the high importance of this pathway for hyper-osmotic (HO) stress tolerance. These abundance changes must be precluded by HO perception and signaling mechanism activation to regulate the expression of *MIPS* and *IMPA1.1* genes. In previous work using a *O. mossambicus* cell line (OmB), a reoccurring osmosensitive enhancer element (OSRE1) in both *MIPS* and *IMPA1.1* was shown to transcriptionally upregulate these enzymes in response to HO stress. The OSRE1 core consensus (5'-GGAAA-3') matches the core binding sequence of the predominant mammalian HO response transcription factor, nuclear factor of activated T-cells (NFAT5). HO challenged OmB cells showed an increase in *NFAT5* mRNA suggesting NFAT5 may contribute to MIB pathway regulation in euryhaline fish. Ectopic expression of wild-type NFAT5 induced an *IMPA1.1* promoter-driven reporter by 5.1-fold ($p < 0.01$). Moreover, expression of dominant negative NFAT5 in HO media resulted in a 47% suppression of the reporter signal ($p<0.005$). Furthermore, reductions of IMPA1.1 (37-49%) and MIPS (6-37%) mRNA abundance were observed in HO challenged NFAT5 knockout cells relative to control cells. Collectively, these multiple lines of experimental evidence establish NFAT5 as a tilapia transcription factor contributing to HO induced activation of the MIB pathway.

NEW & NOTEWORTHY

In our study we use a multi-pronged synthetic biology approach to demonstrate that the fish homolog of the predominant mammalian osmotic stress transcription factor NFAT5 also contributes to the activation of hyperosmolality inducible genes in cells of extremely euryhaline fish. However, in addition

to NFAT5 the presence of other strong osmotically inducible signaling mechanisms is required for full activation of osmoregulated tilapia genes.

Keywords: NFAT5; Hyperosmolality; CRISPR/Cas9; dominant negative mutant; tilapia; synthetic biology

INTRODUCTION

Euryhaline fish acclimate to altered osmotic conditions by regulating their extracellular osmolality and, during severe salinity stress, activation of intracellular enzymes that promote accumulation of compatible organic osmolytes (1). Having one of the widest ranges of salinity tolerance of all fish, *Oreochromis mossambicus* represent an ideal species to study these mechanisms. Physiological stress responses include sensors (the proteins or other molecules that perceive the stress condition), intermediate signal transducers (the molecules that relay the stress signal from the sensors to the effectors), and effector elements (the molecules that mediate the molecular changes allowing persistence during the stress condition). Accumulation of inert intracellular compatible osmolytes such as *myo*-inositol (MI), represents a primary response to relieve osmotic stress caused by extracellular osmolality increases (2–5). Enzymes of the *myo*-inositol biosynthesis (MIB) pathway have been identified as primary proteins that increase in abundance during hyper-osmotic stress in multiple fish species, including tilapia (*Oreochromis* spp.) (3, 6) and European eel (*Anguilla anguilla*) (7). In a tilapia cell line derived from *O. mossambicus* brain tissue (OmB) treated with hyper-osmotic (HO) media, MIB enzyme transcriptional upregulation paralleled that seen in whole animals subjected to HO challenge (8), demonstrating the utility of this model for investigating this pathway. The considerable abundance changes of the MIB pathway enzymes in salinity-stressed cells of tilapia and several species of euryhaline fish illustrates that the regulation of this pathway is a key event for the HO stress response in euryhaline fish. HO induced upregulation of the MIB pathway enzymes requires regulatory enhancer elements that respond to HO conditions. In OmB cells, an osmotic responsive enhancer element (OSRE1) recurs in many locations of the *MIPS* and *IMPA1.1* promoters and was found to be primarily responsible for transcriptional upregulation of these enzymes in HO media (9). Cloning of these OSRE1 enhancers into a minimal promoter expression vector also resulted in strong HO induction of a reporter gene.

The conserved OSRE1 core sequence of 5'-GGAAA-3' represents the core recognition sequence of the Rel homology domain (RHD) (10–13) included in transcription factors commonly associated with cellular stress response signaling, including the nuclear factor of activated T-cell (NFAT) (14) and NF-κB protein families (15, 16). Of the transcription factors belonging to these Rel protein families, NFAT5 is the strongest candidate as an OSRE1 interacting partner since this transcription factor has a well-established role as the primary transcriptional activator of HO responsive genes in mammalian cells (17–20). HO activation of NFAT5 in mammals is achieved by multiple mechanisms, including a localization change (21, 22), post-translational modification (23–25), and increased NFAT5 mRNA abundance (17, 21, 26–29). NFAT5 mRNA abundance increases were also observed in multiple tissues of Atlantic Salmon (*Salmo salar*) exposed to HO challenge (30), suggesting this role is phylogenetically conserved across lower and higher vertebrates.

Effective strategies to establish causal interactions between specific transcription factors and DNA regulatory elements in effector genes include *cis*-element reporter gene expression in combination with either *trans*-factor overexpression (23, 31) or *trans*-factor dominant negative mutant expression (32, 33). A third approach is to generate gene knock-out (KO) animals or cell lines, e.g., by CRISPR/Cas9 gene editing, which is an efficient method for establishing causality between signal transducers and effector mechanisms (34, 35). Disruption of any genetic locus encoding the protein of interest in tilapia cells can be proficiently achieved using a plasmid-based CRISPR/Cas9 system customized for *O. mossambicus* cells (36). In mammalian models NFAT5 KO is usually lethal at early stages of development (37, 38) but NFAT5 KO cell lines are viable, capable of proliferation, and have been used for mechanistic studies of NFAT5 interactions (39–41).

Using the tilapia OmB cell line, the objective of this study was to investigate the role of tilapia NFAT5 for transcriptional HO induction of genes that encode MIB pathway enzymes. This study tested the hypothesis that NFAT5 is necessary for full induction of MIB pathway genes during HO stress.

MATERIALS AND METHODS

Cell lines and maintenance

O. mossambicus OmB wild-type (wt) cells and the engineered Cas9 expressing transgenic OmB cells (Cas9-OmB1) were propagated and maintained according to standard OmB cell culture conditions and protocols as documented in previous reports (8, 36) unless otherwise specified.

Primer design and sequence analysis

All primer design, sequence alignments, and other amino acid/DNA sequence analysis were performed using Geneious Prime software (Version 11.0.3, Biomatters Inc, https://www.geneious.com). All alignments were performed as global alignments with free end gaps.

O. mossambicus NFAT5 mRNA quantitation

To characterize isoform-specific *O. mossambicus NFAT5* mRNA sequences and abundances, OmB cells were exposed to acute HO treatment (media adjusted to 650 mOsm/kg using NaCl) or basal iso-osmotic (IO) control media (315 mOsm/kg) for 6 hours followed by RNA extraction using Invitrogen PureLink RNA Mini Kit (cat# 12183018A). A Qiagen One-step RT-PCR kit (cat# 210210) and gene specific primer pairs for amplicons 1-4 listed in Table 1 were used for cDNA synthesis and PCR amplification of four different regions of the *O. mossambicus* NFAT5 cds. Primers were designed using the XM_005467029 NFAT5 isoform sequence from the *O. niloticus* (taxid: 8128) reference genome. Agarose gel electrophoresis was performed for *O. mossambicus* amplicons 1-4 from both HO and IO treatments.

In a separate experiment, osmotic treatments (HO and IO) and RNA isolation were performed as described above on six replicate 10 cm plates of OmB cells per treatment. Directly after harvesting cells, RNA isolation and cDNA synthesis were performed using Invitrogen Superscript IV (cat.# 18090010) according to manufacturer protocol using 200 ng of template RNA and a 50:50 mix of Oligo-dT and random hexamer primers. Quantitative PCR was performed on 10x dilutions of each cDNA using Promega GoTaq qPCR Master Mix (cat# A6001) on an Applied Biosystems QuantStudio 3 Real-Time PCR system using qPCR primer pairs for *NFAT5* and both β-actin and 18s rRNA as reference genes (RG) as listed in Table 1. The primer pair targeting NFAT5 was designed to flank a 1035 bp intron using *O.*

niloticus (taxid: 8128) *NFAT5* genomic sequence (gene ID # LOC100691255). The RG primer pair sequences were obtained from a previous study (8).

Sequencing and characterization of *O. mossambicus* NFAT5

Using RNA from the HO treated cells, Invitrogen Superscript III (cat.# 18080-044) was used for cDNA synthesis of longer sections of the *O. mossambicus* NFAT5 cds using gene specific primers (NFATX12_R1 for the 5' end of the mRNA transcript and NFATX13_R1 for the 3' end). The cDNA reactions were treated with New England Biolabs RNAse H (cat.# M0297S) followed by PCR amplification to generate amplicons 5 and 6 (for primer pairs see Table 1). Amplicons 8 and 9 were PCR amplified from amplicon 6 as template DNA. DNA sequences for amplicons 1-4, 8, and 9 were obtained from the UC Davis core Sanger sequencing facility (amplicons 8 and 9 were cloned into pBluescript II SK+ first, then sequenced from the plasmid). These sequences were assembled into the complete cds using Geneious software and submitted to the NCBI database.

In silico translation was performed on the constructed *O. mossambicus* NFAT5 cds followed by aa alignment with known functional NFAT5 domains in mammals to identify critical functional domains. These known domains included the nuclear export signal (NES) (22), auxiliary export domain (AED) (42), nuclear localization signal (NLS) (43), DNA binding Rel homology domain (RHD) (32), and transcriptional activation domains (AD1, AD2, and AD3) (23).

Construction of reporter and ectopic expression vectors

An IMPA1.1-EGFP reporter vector was constructed by PCR amplification of a 2700 bp fragment of the *IMPA1.1* promoter. The region of *O. mossambicus* genomic DNA starting at the endogenous start codon on the 3' end and extending to 1065 bp 5' of the predicted TSS (1635 bp between TSS and start codon consisting of exon 1, intron 1, exon 2, intron 2 and the first 36 bp of exon 3) was cloned upstream of the EGFP cds in an EGFP_SV40PA base vector reported previously (36). To confirm HO induced activity of the reporter, two 3.5 cm wells of a plate with 85% confluent OmB cells were transfected with 1 µg of IMPA1.1-EGFP vector. Medium was replaced with either IO (315 mOsm/kg) or HO (650 mOsm/kg) media 24 hours after transfection. Tile scan imaging of the center 10% of each well was performed 24 hours after application of osmotic treatments using a Leica DMi8 inverted microscope with a GFP filter.

To reduce overall plasmid size of the other vectors used in this study, additional truncated recombinant promoters were designed. OmAP(I-)2 and OmEF1a(I-)2 promoters were produced by using their full-length versions (OmBAct and OmEF1a) as PCR templates (36). A reverse primer spanning the 3' end of exon 1 and the 5' end of exon 2 was used for this purpose. This cloning strategy effectively removed intron 1 but maintained the same 5' UTR and the endogenous start codon. Moreover, the Kozak sequence was retained but modified to include a NotI restriction site to provide more cloning options. OmEF1a(I-)2 was cloned into a reporter vector (OmEF1a(I-)2RFP containing the dtomato red fluorescent protein (RFP) cds. This plasmid was used for co-transfection with IMPA1.1-EGFP reporter plasmids to normalize for differences in transfection efficiency and cell density between wells. Another promoter (CMVIE-OmAP(I-)2) was constructed for expression of dominant negative proteins by cloning the cytomegalovirus immediate early enhancer (CMVIE ~300 bp) upstream of the OmAP(I-)2 promoter to improve expression strength. This cloning strategy of fusing interspecies promoters has been demonstrated to be effective (44, 45), including for fish (46).

To generate a dominant negative (DN) NFAT5 cds (NFAT5DN) modeled after mammalian NFAT5DN (32), a truncated NFAT5 cds was PCR amplified using a reverse primer (NFAT5trunc_R; 5'-TTTAAGAAAGTTTTTTCCAATGATGAAGACC-3) designed 3' prime of the RHD but 5' of the AD1 and AD2 domains. This primer was paired with NFAT5_F1 forward primer to PCR amplify (from amplicon 5 as template DNA) a 1332 bp truncated NFAT5 cds including the DNA binding and nuclear localization domains but omitting the transcriptional activation domains. To generate a full wild-type NFAT5 cds (NFAT5WT) the NFAT5DN sequence, amplicon 7 (PCR amplified from amplicon 5, spanning exon 7 to exon 12), and the C-terminal fragments (amplicons 8 and 9 containing exons 12-13 sub-cloned from pBluescript II SK+ plasmid) were assembled into a new plasmid using standard restriction enzyme techniques. The NFAT5DN cds was cloned into a plasmid driven by the CMVIE-OmAP(I-)2 promoter generating the NFAT5DN vector. The full length wild-type (WT) cds was cloned into a plasmid driven by the OmAP(I-)2 promoter to generate the NFAT5WT vector. The first 1332 base pairs of Cas9 cds were also cloned into a plasmid driven by the CMVIE-OmAP(I-)2 promoter to be used as an overexpression vector (OE) that controls for non-specific deleterious effects caused by ectopic protein expression (47).

EGFP/RFP Reporter Assays

For the NFAT5DN inhibition experiments, transfection reactions consisted of 1000 ng expression vector, 100 ng IMPA1.1-EGFP reporter, and 100 ng RFP normalizer plasmids. Three variations of expression vector were used: 100% OE control vector, 50% OE control vector plus 50% NFAT5DN vector, and 100% NFAT5DN vector. Four replicates of these plasmid combinations were used for each HO (650 mOsm/kg) and IO (315 mOsm/kg) control treatments. Plasmid transfections of cells were performed using Promega ViaFect (cat.# E4981) followed by 48 hour exposure to either HO or IO conditions after transfection. Tile scan imaging of the center 10% of each well was performed 24 hours after HO and IO treatments. For the NFAT5WT activation experiments, plasmid complexes were prepared consisting of 500 ng expression vector, 50 ng IMPA1.1-EGFP reporter, and 50 ng RFP normalizer plasmids. Two variations of expression vector were used: 100% OE control vector, and 100% NFAT5WT vector. Two replicates were used per treatment group with each replicate consisting of one 12-well plate of OmB cells. Tile scan imaging was performed on the center 20% of each well 24 hours after transfection. All images were generated using a 20X objective and both GFP (30 ms exposure) and TXR (20 ms exposure for RFP) filters as composite tile scans using a Leica DMi8 inverted microscope. Total fluorescence intensity per filter was quantified using the LASX Navigator analysis tool (Leica Application Suite X Version 3.0.4 software). Reporter activity is expressed as relative fluorescence intensity (RFI = total EGFP fluorescence intensity/ total RFP fluorescence intensity).

Generation of NFAT5 KO cell lines

Non-essential (NE) control KO lines, gRNA selection process, and methods for generation and genotyping of KO cell lines were chosen and performed as described previously(48). The NFAT5 amino acid sequences for *O. niloticus* (XP_005467085), *Oryzias latipes* (XP_011487371), and *Fundulus heteroclitus* (XP_021177424.2) were aligned to find the most conserved regions within the first third of the coding sequence that would have the highest probability of gene product disruption by CRISPR/Cas9 targeting. The corresponding nucleotide sequences of these regions were entered into the online CRISPOR gRNA selection algorithm (49) to find candidate gRNAs with the highest predicted specificity (lowest potential of off-target effects) and efficiency (highest potential to cleave target site) scores. Based on these scores, eight gRNAs were selected for *in vivo* empirical testing of mutational efficiency. Expression plasmids for each candidate gRNA were constructed and transfected into Cas9-OmB1 cells,

followed by hygromycin B selection, direct PCR of test amplicons including the gRNA targeted region, Sanger sequencing, and INDEL% quantification of the resulting chromatogram using the online TIDE mutational efficiency algorithm (50). The top three INDEL% scoring guides were used to repeat CRISPR/Cas9 treatment of Cas9-OmB1 cells followed by low density seeding of hygromycin B selected cells into 96-well plates. Selected wells were genotyped by direct PCR and Sanger sequencing of the corresponding test amplicon followed by input of the chromatogram into the online DECODR algorithm (51). Selected genotypes showing a maximum of two alleles all with 100% frameshift mutation were propagated and genotyped again after multiple passages. One genotype for each gRNA was selected based on maintenance of the original genotype and highest R^2 model fit for the DECOCDR algorithm was selected for subsequent experiments.

Quantitative PCR of IMPA1.1 and MIPS in NFAT5 KO cells

The three NFAT5 KO lines and three NE control KO lines (NANOS3, MSTN T5, and TYR T1) from previous work (52) were grown to ~90% confluency in 6 cm plates followed by acute replacement of media with either 650 mOsm/kg HO or control 315 mOsm/kg IO media. Cell harvest and RNA isolation was performed 24 hours after dosing followed by cDNA synthesis and quantitative PCR as described in the previous section except: a 1000x dilution was used for 18s rRNA RG. The target gene primer pairs used were IMPA1 and MIPS-250 from a previous study (8). For each combination (target gene, RG, and osmotic treatment) the fold change between the NFAT5 KO and NE KO control groups was calculated using the $2^{-\Delta\Delta Ct}$ method (53, 54).

Statistical Analysis

All statistical analyses were performed using Rstudio version 2021.09.1. One tailed Welch and two sample t-tests were performed on all relative mRNA abundance comparisons and for determining the effect of NFAT5WT activation on IMPA1.1-EGFP reporter induction. Linear regression was used to model the effect of NFAT5DN inhibition on HO induction of the IMPA1.1-EGFP reporter. All quantitative data is reported as means with variation represented as standard deviation (SD).

RESULTS

RT-PCR of NFAT5

Qualitative assessment of PCR amplicon images after gel electrophoresis of the different NFAT5 cds segments yields consistently brighter bands from HO treated cells compared to IO controls across all segments (Figure 1A). Quantitative PCR of NFAT5 mRNA abundance confirms these visual approximations by yielding mean mRNA abundance values of 2.80E-03 (SD 9.59E-04) for IO and 1.07E-02 (SD 1.96E-03) for HO conditions and a statistically significant mean fold change of 3.87 (p value = 1.789e-05) in HO treated cells relative to iso-osmotic treated controls (Figure 1B).

Characterization of HO induced NFAT5

The assembled *O. mossambicus NFAT5* cds sequence from HO treated cells (NCBI accession # MW075269.1) was aligned with the predicted *O. niloticus NFAT5* isoform with all possible exons (XM_005467029) to identify the exon splicing pattern and any sequence differences between these two tilapia species (Figure 1C). When compared to the predicted *O. niloticus NFAT5* isoform XM_005467029, the predicted *O. mossambicus* HO induced *NFAT5* transcript (MW075269.1) is missing exon 2 and contains the shorter 65 bp version of exon 11 (Figure 1C). The mammalian NFAT5 domain aa sequences

aligned to the MW075269.1 predicted aa sequence with pairwise % identities of NES = 81.8, AED = 76.9, NLS = 70.6, RHD = 82.2, AD2 = 32.1, and AD3 = 40.9. The AD1 domain was omitted from MW075269.1 along with exon 2 but aligned to *O. niloticus* NFAT5 isoform XP_005467085 with 60.7 pairwise % identity. All domains aligned in the same relative position as previously reported for mammals (23, 55)(Figure 1D).

Construction and validation of reporter plasmids

Based on the *O. niloticus* reference genome, the selected regulatory *IMPA1.1* promoter region should have been 4086 bp, however a 1386 bp section in the intron between exons 2 and 3 was omitted from the region PCR amplified from *O. mossambicus* genomic DNA, resulting in the 2700 bp region that was cloned into the EFGP_SV40 PA reporter vector (Figure 2A). HO responsiveness of the reporter vector was qualitatively confirmed from tile scan images post transfection and HO treatment with notably higher EGFP intensity of the HO treated cells (Figure 2B). The engineered OmEF1a(I-)2 promoter (Figure 2C) showed strong, stable RFP expression (Figure 2D).

Interaction between NFAT5DN or NFAT5WT with IMPA1.1 reporter

The engineered CMVIE-OmAP(I-)2 promoter (Figure 3A) was effective in producing sufficient NFAT5DN quantities as HO RFI induction of the IMPA1.1-EGFP reporter decreased linearly with increasing concentration of NFAT5DN (p-value = 0.00269) amounting to a 47% reduction from no NFAT5DN present to the highest NFAT5DN concentration (Figure 3B): 0 µg NFAT5DN mean RFI = 1.068 (SD 0.210), 0.5 µg NFAT5DN mean RFI = 0.916 (SD 0.107), and 1 µg NFAT5DN mean RFI = 0.565 (SD 0.207). In IO media, IMPA1.1-EGFP reporter the mean RFI in NFAT5WT transfected cells of 0.690 (SD 0.044) was significantly greater (5.1 fold, $p < 0.01$) compared to the mean RFI of 0.140 (SD 0.018) in cells transfected with the OE control vector (Figure 3C).

CRISPR/Cas9 gRNA design and testing

The interspecies NFAT5 aa sequence alignments identified the most highly conserved region as between aa 320 and 450 of the *O. niloticus* NFAT5 protein (XP_005467085) (Figure 4A). This region corresponded to exons 4 through 6 of the *O. niloticus NFAT5* genomic sequence (gene ID # LOC100691255), in which the candidate gRNAs were found by CRISPOR algorithm search (Figure 4B). The top eight selected candidate gRNAs all yielded high MIT specificity (92 or greater) and Doench efficiency (45 or greater) scores (Table 2). The three gRNAs with the highest TIDE mutational efficiency scores from *in vivo* empirical testing were T3 (60.4%), T5 (51.9%), and T7 (56.1%).

Generation of NFAT5 KO clonal lines

All gRNA targets yielded at least one clonal genotype with 100% frameshift mutation that remained constant from initial genotyping to the end of the experiment after multiple passages. The selected clones for subsequent experiments all maintained a high R^2 DECODR model fit of 0.94 or greater throughout the entire experiment (Figure 5).

IMPA1.1 and MIPS mRNA abundances in NFAT5 KO cells exposed to IO and HO conditions

Quantitative PCR was performed on the NFAT5 KO and NE KO control lines after 24 hours exposure to HO challenge (650 mOsm/kg) or IO control (315 mOsm/kg) media with primer pairs targeting IMPA1.1 and MIPS transcripts and using both β-actin and 18s ribosomal RNA as RG. In IO control media, the relative mean mRNA abundance values for each group were: NE KO control = 2.58E-04 (SD 1.25E-04) and NFAT5KO = 4.10E-04 (SD 3.22E-04) for MIPS using β-actin RG, NE KO control = 3.39E-05 (SD 1.61E-

05) and NFAT5KO = 4.04E-05 (SD 2.16E-05) for MIPS using 18s RG, NE KO control = 4.67E-03 (SD 3.70E-03) and NFAT5KO = 3.77E-03 (SD 3.37E-03) for IMPA1.1 using β-actin RG, NE KO control = 6.00E-04 (SD 4.75E-04) and NFAT5KO = 4.16E-04 (SD 4.12E-04) for IMPA1.1 using 18s RG. There was no significant difference between NFAT5KO and NE KO controls in IO media for both MIPS mean mRNA relative abundance (β-actin RG: 1.59 fold change, p-value= 0.7449 and 18s rRNA RG: 1.19 fold change, p-value= 0.6508) and IMPA1.1 mRNA relative abundance (β-actin RG: 0.81 fold change, p-value= 0.3845 and 18s rRNA RG: 0.69 fold change, p-value= 0.3204) using either reference gene (Figure 6). In HO media, the relative mean mRNA abundance values for each group were: NE KO control = 5.39E-03 (SD 2.53E-03) and NFAT5KO = 5.09E-03 (SD 2.13E-03) for MIPS using β-actin RG, NE KO control = 3.93E-04 (SD 2.02E-04) and NFAT5KO = 2.46E-04 (SD 7.59E-05) for MIPS using 18s RG, NE KO control = 1.772 (SD 0.545) and NFAT5KO = 1.292 (SD 0.044) for IMPA1.1 using β-actin RG, NE KO control = 1.26E-01 (SD 2.41E-02) and NFAT5KO = 6.41E-02 (SD 5.56E-03) for IMPA1.1 using 18s RG. For both reference genes, this yielded reductions in MIPS mRNA abundance (β-actin RG: 0.94 fold change, p-value= 0.4404, Figure 6A, and 18s rRNA RG: 0.63 fold change, p-value= 0.1677, Figure 6B) and IMPA1.1 mRNA abundance (β-actin RG: 0.73 fold change, p-value= 0.1331, Figure 6C, and 18s rRNA RG: 0.51 fold change, p-value= 0.02036, Figure 6D) in NFAT5KO cells relative to NE KO control lines.

DISCUSSION

Previous work with MIB pathway enzyme promoters suggested these enzymes are influenced by a homolog of the mammalian HO stress regulator NFAT5(9). In addition, NFAT5 induction in response to HO stress has been observed in all vertebrate classes investigated thus far, i.e., in mammals (56, 57), amphibians (58), and fish(30). Conservation of this role from even earlier in phylogenetic history is implied by HO responsiveness of NAFT5 from *Ciona robusta*, a primitive chordate , when expressed in a human cell line (59). In mammalian models, extensive work has been done on the role of NFAT5 for HO responsive gene expression, where NFAT5 accounts for the majority of HO induced transcriptional changes (19, 56, 57, 60). Considering the phylogenetic conservation of HO responsive NFAT5 signaling, we hypothesized that highly euryhaline fish species like *O. mossambicus* also possess this regulatory mechanism. This study uses the tilapia OmB cell line model to provide insight in the role of NFAT5 for osmotic stress signaling in *O. mossambicus* and other euryhaline fishes.

It is common for different gene suppression techniques to yield a different phenotype for the same target gene (61). Therefore, applying multiple strategies yields the most robust results. Ectopic expression of DN TFs, i.e., TFs in which the TAD is deleted but the DBD is maintained (33), is an effective strategy to evaluate interactions with DNA regulatory elements and has been a critical tool in deciphering the functions and interactions of other RHD transcription factors (32, 62, 63). However, DN proteins require precise engineering in order to function as intended and thus when using a new DN protein it may not be certain to what degree observations are due to endogenous interactions between the proteins in question or the effectiveness of the DN design. We used characterization of the predicted XM_005467029 aa sequence using domain information and validated NFATDN design from mammalian studies (32) to maximize the potential for *O. mossambicus* NFAT5DN intended functionality. Over-expression of TFs has been historically useful in elucidating protein function (31, 64). However, TFs can bind to DNA non-specifically (65, 66) and abnormally high concentration can result in increased global transcription (67, 68) leading to erroneous transcriptionally induced phenotypes. This potential

confounding factor was accounted for by normalization through co-transfection of the IMPA1.1-EGFP reporter with the RFP vector which would also be affected by non-specific TF activity. CRISPR/Cas9 mediated editing is another efficient method for target gene disruption but careful interpretation of the effect is required due to the potential of cellular changes not relevant to the phenotype in question caused by unknown off target effects (69). Here, replication with multiple NFAT5 KO clones obtained from different gRNAs was used to control for this potential pitfall. Collectively, these approaches can provide compelling evidence in deciphering the interactions between NFAT5 and its target genes.

The capability of NFAT5 to induce the IMPA1.1 promoter was demonstrated by the statistically significant induction of the IMPA1.1-EGFP reporter by NFAT5WT in IO conditions. The HO induced upregulation of *NFAT5* mRNA abundance observed by qRT-PCR in tilapia OmB cells was also highly significant, consistent with the typical response of HO exposed mammalian cells (17, 56, 70). Collectively, this established high plausibility that NFAT5 is at least partially responsible for the HO induced increase in IMPA1.1 mRNA abundance that is consistently observed in tilapia cells (3, 6, 8, 71).

Here we use dominant negative and gene KO approaches to establish causality between NFAT5 and MIB enzyme regulation. The NFAT5DN and NFAT5KO results for HO regulation of IMPA1.1 are consistent with each other and the result of NFAT5WT overexpression in cells exposed to IO. The continuity of these results instills high confidence in the methodologies and the observed results. Collectively, our results indicate that tilapia NFAT5 is partly responsible for *IMPA1.1* (37 – 49%) and MIPS (6 - 37%) transcriptional induction during HO stress. Considering the magnitude at which these genes are HO induced there is still a very substantial amount of HO induced gene activation present despite disrupted NFAT5 signaling. This result suggests that in tilapia cells other osmo-responsive signaling networks are strongly induced by the HO stress. Since *O. mossambicus* and other euryhaline fishes encounter osmotic gradients in an aqueous ambient environment, and can sustain more rapid and extreme changes in plasma osmolalities (3, 72, 73), a much wider range of tissues and cell types are subjected to a more dynamic range of osmotic exposure. This may necessitate complementary signaling mechanisms to account for these more diverse osmotic challenges.

The *MIPS* and *IMPA1.1* promoter regions contain a similar copy numbers of the OSRE1 enhancer (9), and yet, a lesser relative impact of NFAT5KO on *MIPS* abundance was observed compared to *IMPA1.1*. Although the consensus OSRE1 core was present in all of these *cis*-elements, the overall enhancer sequence was highly variable. NFAT5 has the most stringent binding sequence of all the NFATs and its binding affinity is highly affected by core adjacent sequence (74, 75). Consequently, the relative influence NFAT5 has on transcription is dependent on the collective sequence dependent binding affinity of all the OSRE1 elements present in the promoter. Although not generally associated with HO signaling, the calcineurin regulated NFAT1-4 proteins are possible additional interacting partners with OSRE1 as there is high overlap in binding sequence between all the NFATs and there have been other accounts of calcineurin based NFAT signaling in response to HO stress. In immortalized murine renal collecting duct cells calcineurin mediated regulation of aquaporin 2 expression was demonstrated in response to HO stress (76). This response would require an increase of intracellular Ca^{2+} which is commonly associated with hypo-osmotic response (1, 77), however, conflicting reports exist that it can also be a HO response (78, 79). Like most promoters which contain many different *cis* elements responsive to a variety of regulators, the *IMPA1.1* promoter contains several HO responsive regions lacking an OSRE1 (9) representing potential *cis* elements that interact with parallel NFAT independent HO signaling pathways. The ubiquitous c-Myc (80), osmotic stress transcription factor 1 (Ostf1) (81), and

CCAAT/enhancer binding protein (C/EBP) (82) are among other transcription factors associated with the HO stress response in fish and may interact with NFAT5 to achieve full HO induction of MIB pathway genes.

Despite the evidence supporting NFAT5 is only responsible for approximately half of HO induced IMPA1.1 promoter activity, the effect size observed by ectopic NFAT5WT expression seems comparatively low. HO treatment typically leads to IMPA1.1 mRNA abundances in excess of several hundred-fold which is substantially higher than the 5.1-fold induction of the IMPA1.1-EGFP reporter by NFAT5WT. The disparity seems even more striking when considering the NFAT5WT was expressed from a β-actin promoter likely leading to NFAT5 levels in excess of what occurs naturally. This discrepancy can be reconciled by the post translational regulation of NFAT5. Since NFAT5WT overexpression in this study was performed in IO conditions, any localization or activity effects caused by HO conditions were not represented in this result.

In mammalian models, subcellular distribution of NFAT5 is controlled by an N-terminal regulatory domain (NTD) containing a N-terminal NES, followed by AD1 (23), the hypo-osmotic responsive AED (42), and the potent HO responsive NLS (43). In basal IO conditions, mammalian NFAT5 has a constitutive distribution throughout both the cytoplasm and the nucleus held in equilibrium by this region (55, 75). HO conditions induce strong NFAT5 nuclear enrichment (42, 55, 83), which is mediated by HO activation of the NLS (43). Considering the highly conserved N-terminal NFAT5 domain, the mechanism of HO regulation of *O. mossambicus* NFAT5 is likely very similar to that observed in mammalian models. In addition to nuclear localization, transcriptional activity is also highly HO induced by multiple post translational modifications to the TADs (AD1, AD2, and AD3) and other accessory modulating domains (23–25). In HO treated NFAT5 TADs isolated from the NTD, activity increases of several magnitudes have been observed (23, 25). Interestingly, exon 2 which contains the AD1 activation domain is excised from the predominant HO induced NFAT5 isoform observed in this study. Although weaker than the other NFAT5 ADs, mammalian AD1 has demonstrated intrinsic transcriptional activity and an ability to synergistically enhance the activation strength of the other NFAT5 ADs up to two-fold (23). Excision of exon 2 from the HO induced form of *O. mossambicus* NFAT5 seems counterintuitive, especially considering the two nuclear export signals (NES and AED) flanking exon 2 are still maintained in the transcript. Conformational change leading to increased activity of mammalian NFAT5 in response to elevated ions has been reported (84). This conformational change might have a suppressive effect on one or both export signals. Therefore, it is possible omission of exon 2 in the HO induced NFAT5 isoform from this study results in a structural change that functionally replicates this effect. Collectively, these considerations support that full *O. mossambicus* NFAT5 HO influence is a combination of changes in NFAT5 abundance, localization, and activity.

Perspectives and Significance

Although a role of NFAT5 in fish salinity tolerance has been implicated, this study is the first to establish causality between NFAT5 and HO induced differential gene expression in fish cells. The work described here provides important new insights on the mechanisms of fish salinity tolerance, especially those influenced by NFAT5. This work has produced new valuable tools and methodologies such as dominant negative expression systems and NFAT5 KO cell lines to further evaluate the role of NFAT5 and other complimentary regulators in HO tolerance and for other physiological functions of euryhaline fishes.

By accounting for weaknesses of each method and using a very comprehensive multifaceted approach composed of distinct methods and numerous controls that all supported the same results, we have accumulated solid support for the following conclusions: *O. mossambicus* NFAT5 mRNA abundance is elevated during HO stress, specifically a predominant isoform that is missing the AD1 containing exon 2. This isoform is able to localize to the nucleus and induce transcription in the absence of HO induction indicating its capability for maintaining basal activity under IO conditions. In OmB cells, NFAT5 has a clear role in the regulation of the highly HO transcriptionally induced *IMPA1.1* and *MIPS* genes. Disruption of NFAT5 results in up to 49% and 37% reduction of HO induced mRNA abundance for IMPA1.1 and MIPS, respectively. This contribution of tilapia NFAT5 to HO target gene induction is less than what is typically observed in mammalian models. Therefore, euryhaline fish such as tilapia must have a more elaborate HO response signaling network with other strongly induced signaling pathways that are activated jointly with NFAT5 signaling pathways during HO stress.

DATA AVAILABILITY

Raw data can be made available upon request.

ACKNOWLEDGMENTS

The authors thank Leah MacNiven for assisting with fluorescent imaging and Amber Yiao for help in primer design of NFAT5 qRT-PCR primers.

GRANTS

National Science Foundation, Grant/Award Number: IOS- 2209383.
US-Israel Binational Agricultural Research and Development Fund, Grant/Award Number: IS-5358-21.

DISCLOSURES

The authors have no conflicts of interest to disclose.

AUTHOR CONTRIBUTIONS

J.H. and D.K. conceived and designed research, J.H. performed experiments, analyzed data, interpreted results of experiments, prepared figures, and drafted manuscript. J.H., D.K., and A.C. edited and revised manuscript. J.H., D.K., and A.C. approved final version of manuscript.

REFERENCES

1. **Kültz D**. The combinatorial nature of osmosensing in fishes. *Physiology (Bethesda)* 27: 259–275, 2012. doi: 10.1152/physiol.00014.2012.

2. **Bagnasco S**, **Balaban R**, **Fales HM**, **Yang YM**, **Burg M**. Predominant osmotically active organic solutes in rat and rabbit renal medullas. *J Biol Chem* 261: 5872–5877, 1986.

3. **Gardell AM**, **Yang J**, **Sacchi R**, **Fangue NA**, **Hammock BD**, **Kültz D**. Tilapia (*Oreochromis mossambicus*) brain cells respond to hyperosmotic challenge by inducing *myo*-inositol biosynthesis. *J Exp Biol* 216: 4615–4625, 2013. doi: 10.1242/jeb.088906.

4. **Yancey PH**, **Clark ME**, **Hand SC**, **Bowlus RD**, **Somero GN**. Living with water stress: evolution of osmolyte systems. *Science* 217: 1214–1222, 1982. doi: 10.1126/science.7112124.

5. **Michell RH**. Inositol derivatives: evolution and functions. *Nat Rev Mol Cell Biol* 9: 151–161, 2008. doi: 10.1038/nrm2334.

6. **Sacchi R**, **Li J**, **Villarreal F**, **Gardell AM**, **Kültz D**. Salinity-induced regulation of the *myo*-inositol biosynthesis pathway in tilapia gill epithelium. *J Exp Biol* 216: 4626–4638, 2013. doi: 10.1242/jeb.093823.

7. **Kalujnaia S**, **Gellatly SA**, **Hazon N**, **Villasenor A**, **Yancey PH**, **Cramb G**. Seawater acclimation and inositol monophosphatase isoform expression in the European eel (*Anguilla anguilla*) and Nile tilapia (*Orechromis niloticus*). *Am J Physiol Regul Integr Comp Physiol* 305: R369-384, 2013. doi: 10.1152/ajpregu.00044.2013.

8. **Gardell AM**, **Qin Q**, **Rice RH**, **Li J**, **Kültz D**. Derivation and osmotolerance characterization of three immortalized tilapia (*Oreochromis mossambicus*) cell lines. *PLoS One* 9: e95919, 2014. doi: 10.1371/journal.pone.0095919.

9. **Wang X**, **Kültz D**. Osmolality/salinity-responsive enhancers (OSREs) control induction of osmoprotective genes in euryhaline fish. *Proc Natl Acad Sci U S A* 114: E2729–E2738, 2017. doi: 10.1073/pnas.1614712114.

10. **Senger K**, **Armstrong GW**, **Rowell WJ**, **Kwan JM**, **Markstein M**, **Levine M**. Immunity regulatory DNAs share common organizational features in *Drosophila*. *Mol Cell* 13: 19–32, 2004. doi: 10.1016/s1097-2765(03)00500-8.

11. **Kunsch C**, **Ruben SM**, **Rosen CA**. Selection of optimal kappa B/Rel DNA-binding motifs: interaction of both subunits of NF-kappa B with DNA is required for transcriptional activation. *Mol Cell Biol* 12: 4412–4421, 1992. doi: 10.1128/mcb.12.10.4412-4421.1992.

12. **Ghosh S**, **May MJ**, **Kopp EB**. NF-kappa B and Rel proteins: evolutionarily conserved mediators of immune responses. *Annu Rev Immunol* 16: 225–260, 1998. doi: 10.1146/annurev.immunol.16.1.225.

13. **Northrop JP**, **Ho SN**, **Chen L**, **Thomas DJ**, **Timmerman LA**, **Nolan GP**, **Admon A**, **Crabtree GR**. NF-AT components define a family of transcription factors targeted in T-cell activation. *Nature* 369: 497–502, 1994. doi: 10.1038/369497a0.

14. **Rao A**, **Luo C**, **Hogan PG**. Transcription factors of the NFAT family: regulation and function. *Annu Rev Immunol* 15: 707–747, 1997. doi: 10.1146/annurev.immunol.15.1.707.

15. **Chen Y-Q**, **Sengchanthalangsy LL**, **Hackett A**, **Ghosh G**. NF-κB p65 (RelA) homodimer uses distinct mechanisms to recognize DNA targets. *Structure* 8: 419–428, 2000. doi: 10.1016/S0969-2126(00)00123-4.

16. **Ghosh G**, **Duyne GV**, **Ghosh S**, **Sigler PB**. Structure of NF-κB p50 homodimer bound to a κB site. *Nature* 373: 303–310, 1995. doi: 10.1038/373303a0.

17. **Kino T**, **Takatori H**, **Manoli I**, **Wang Y**, **Tiulpakov A**, **Blackman MR**, **Su YA**, **Chrousos GP**, **DeCherney AH**, **Segars JH**. Brx mediates the response of lymphocytes to osmotic stress through the activation of NFAT5. *Sci Signal* 2: ra5, 2009. doi: 10.1126/scisignal.2000081.

18. **Woo SK**, **Lee SD**, **Na KY**, **Park WK**, **Kwon HM**. TonEBP/NFAT5 stimulates transcription of HSP70 in response to hypertonicity. *Mol Cell Biol* 22: 5753–5760, 2002. doi: 10.1128/MCB.22.16.5753-5760.2002.

19. **López-Rodríguez C**, **Antos CL**, **Shelton JM**, **Richardson JA**, **Lin F**, **Novobrantseva TI**, **Bronson RT**, **Igarashi P**, **Rao A**, **Olson EN**. Loss of NFAT5 results in renal atrophy and lack of tonicity-responsive gene expression. *Proc Natl Acad Sci U S A* 101: 2392–2397, 2004. doi: 10.1073/pnas.0308703100.

20. **Ito T**, **Fujio Y**, **Hirata M**, **Takatani T**, **Matsuda T**, **Muraoka S**, **Takahashi K**, **Azuma J**. Expression of taurine transporter is regulated through the TonE (tonicity-responsive element)/TonEBP (TonE-binding protein) pathway and contributes to cytoprotection in HepG2 cells. *Biochem J* 382: 177–182, 2004. doi: 10.1042/BJ20031838.

21. **Woo SK**, **Dahl SC**, **Handler JS**, **Kwon HM**. Bidirectional regulation of tonicity-responsive enhancer binding protein in response to changes in tonicity. *Am J Physiol Renal Physiol* 278: F1006-1012, 2000. doi: 10.1152/ajprenal.2000.278.6.F1006.

22. **Tong EHY**, **Guo J-J**, **Huang A-L**, **Liu H**, **Hu C-D**, **Chung SSM**, **Ko BCB**. Regulation of nucleocytoplasmic trafficking of transcription factor OREBP/TonEBP/NFAT5. *J Biol Chem* 281: 23870–23879, 2006. doi: 10.1074/jbc.M602556200.

23. **Lee SD**, **Colla E**, **Sheen MR**, **Na KY**, **Kwon HM**. Multiple domains of TonEBP cooperate to stimulate transcription in response to hypertonicity. *J Biol Chem* 278: 47571–47577, 2003. doi: 10.1074/jbc.M308795200.

24. **Choi SY**, **Lee-Kwon W**, **Kwon HM**. The evolving role of TonEBP as an immunometabolic stress protein. *Nat Rev Nephrol* 16: 352–364, 2020. doi: 10.1038/s41581-020-0261-1.

25. **Ferraris JD**, **Williams CK**, **Persaud P**, **Zhang Z**, **Chen Y**, **Burg MB**. Activity of the TonEBP/OREBP transactivation domain varies directly with extracellular NaCl concentration. *Proc Natl Acad Sci U S A* 99: 739–744, 2002. doi: 10.1073/pnas.241637298.

26. **Ko BCB**, **Turck CW**, **Lee KWY**, **Yang Y**, **Chung SSM**. Purification, Identification, and Characterization of an Osmotic Response Element Binding Protein. *Biochem Biophys Res Commun* 270: 52–61, 2000. doi: 10.1006/bbrc.2000.2376.

27. **Navarro P**, **Chiong M**, **Volkwein K**, **Moraga F**, **Ocaranza MP**, **Jalil JE**, **Lim SW**, **Kim J-A**, **Kwon HM**, **Lavandero S**. Osmotically-induced genes are controlled by the transcription factor TonEBP in cultured cardiomyocytes. *Biochem Biophys Res Commun* 372: 326–330, 2008. doi: 10.1016/j.bbrc.2008.05.067.

28. **Tsai T-T**, **Guttapalli A**, **Agrawal A**, **Albert TJ**, **Shapiro IM**, **Risbud MV**. MEK/ERK signaling controls osmoregulation of nucleus pulposus cells of the intervertebral disc by transactivation of TonEBP/OREBP. *J Bone Miner Res* 22: 965–974, 2007. doi: 10.1359/jbmr.070322.

29. **Lee JH**, **Kim M**, **Im YS**, **Choi W**, **Byeon SH**, **Lee HK**. NFAT5 induction and its role in hyperosmolar stressed human limbal epithelial cells. *Invest Ophthalmol Vis Sci* 49: 1827–1835, 2008. doi: 10.1167/iovs.07-1142.

30. **Lorgen M**, **Jorgensen EH**, **Jordan WC**, **Martin SAM**, **Hazlerigg DG**. NFAT5 genes are part of the osmotic regulatory system in Atlantic salmon (*Salmo salar*). *Mar Genomics* 31: 25–31, 2017. doi: 10.1016/j.margen.2016.06.004.

31. **Prelich G**. Gene overexpression: uses, mechanisms, and interpretation. *Genetics* 190: 841–854, 2012. doi: 10.1534/genetics.111.136911.

32. **Miyakawa H**, **Woo SK**, **Dahl SC**, **Handler JS**, **Kwon HM**. Tonicity-responsive enhancer binding protein, a rel-like protein that stimulates transcription in response to hypertonicity. *Proc Natl Acad Sci U S A* 96: 2538–2542, 1999. doi: 10.1073/pnas.96.5.2538.

33. **Brown PH**, **Alani R**, **Preis LH**, **Szabo E**, **Birrer MJ**. Suppression of oncogene-induced transformation by a deletion mutant of c-jun. *Oncogene* 8: 877–886, 1993.

34. **Cortez JT**, **Montauti E**, **Shifrut E**, **Gatchalian J**, **Zhang Y**, **Shaked O**, **Xu Y**, **Roth TL**, **Simeonov DR**, **Zhang Y**, **Chen S**, **Li Z**, **Woo JM**, **Ho J**, **Vogel IA**, **Prator GY**, **Zhang B**, **Lee Y**, **Sun Z**, **Ifergan I**, **Van Gool F**, **Hargreaves DC**, **Bluestone JA**, **Marson A**, **Fang D**. CRISPR screen in regulatory T cells reveals modulators of Foxp3. *Nature* 582: 416–420, 2020. doi: 10.1038/s41586-020-2246-4.

35. **de Almeida M**, **Hinterndorfer M**, **Brunner H**, **Grishkovskaya I**, **Singh K**, **Schleiffer A**, **Jude J**, **Deswal S**, **Kalis R**, **Vunjak M**, **Lendl T**, **Imre R**, **Roitinger E**, **Neumann T**, **Kandolf S**, **Schutzbier M**, **Mechtler K**, **Versteeg GA**, **Haselbach D**, **Zuber J**. AKIRIN2 controls the nuclear import of proteasomes in vertebrates. *Nature* 599: 491–496, 2021. doi: 10.1038/s41586-021-04035-8.

36. **Hamar J**, **Kültz D**. An efficient vector-based CRISPR/Cas9 system in an *Oreochromis mossambicus* cell line using endogenous promoters. *Sci Rep* 11: 7854, 2021. doi: 10.1038/s41598-021-87068-3.

37. **Mak MC**, **Lam KM**, **Chan PK**, **Lau YB**, **Tang WH**, **Yeung PKK**, **Ko BCB**, **Chung SMS**, **Chung SK**. Embryonic Lethality in Mice Lacking the Nuclear Factor of Activated T Cells 5 Protein Due to Impaired Cardiac Development and Function. *PLOS ONE* 6: e19186, 2011. doi: 10.1371/journal.pone.0019186.

38. **Go WY**, **Liu X**, **Roti MA**, **Liu F**, **Ho SN**. NFAT5/TonEBP mutant mice define osmotic stress as a critical feature of the lymphoid microenvironment. *Proc Natl Acad Sci U S A* 101: 10673–10678, 2004. doi: 10.1073/pnas.0403139101.

39. **Chernyakov D**, **Groß A**, **Fischer A**, **Bornkessel N**, **Schultheiss C**, **Gerloff D**, **Edemir B**. Loss of RANBP3L leads to transformation of renal epithelial cells towards a renal clear cell carcinoma like phenotype. *J Exp Clin Cancer Res* 40: 226, 2021. doi: 10.1186/s13046-021-01982-y.

40. **Kim G-N**, **Hah Y-S**, **Seong H**, **Yoo W-S**, **Choi M-Y**, **Cho H-Y**, **Yun SP**, **Kim S-J**. The Role of Nuclear Factor of Activated T Cells 5 in Hyperosmotic Stress-Exposed Human Lens Epithelial Cells. *Int J Mol Sci* 22, 2021. doi: 10.3390/ijms22126296.

41. **Kang K**, **Huang L**, **Li Q**, **Liao X**, **Dang Q**, **Yang Y**, **Luo J**, **Zeng Y**, **Li L**, **Gou D**. An improved Tet-on system in microRNA overexpression and CRISPR/Cas9-mediated gene editing. *J Anim Sci Biotechnol* 10: 43, 2019. doi: 10.1186/s40104-019-0354-5.

42. **Xu S**, **Wong CCL**, **Tong EHY**, **Chung SSM**, **Yates JR III**, **Yin Y**, **Ko BCB**. Phosphorylation by Casein Kinase 1 Regulates Tonicity-induced Osmotic Response Element-binding Protein/Tonicity Enhancer-binding Protein Nucleocytoplasmic Trafficking *. *J Biol Chem* 283: 17624–17634, 2008. doi: 10.1074/jbc.M800281200.

43. **Kwon MS**, **Lee SD**, **Kim J-A**, **Colla E**, **Choi YJ**, **Suh P-G**, **Kwon HM**. Novel nuclear localization signal regulated by ambient tonicity in vertebrates. *J Biol Chem* 283: 22400–22409, 2008. doi: 10.1074/jbc.M710550200.

44. **Zúñiga RA**, **Gutiérrez-González M**, **Collazo N**, **Sotelo PH**, **Ribeiro CH**, **Altamirano C**, **Lorenzo C**, **Aguillón JC**, **Molina MC**. Development of a new promoter to avoid the silencing of genes in the production of recombinant antibodies in chinese hamster ovary cells. *J of Biol Eng* 13: 59, 2019. doi: 10.1186/s13036-019-0187-y.

45. **Hitoshi N**, **Ken-ichi Y**, **Jun-ichi M**. Efficient selection for high-expression transfectants with a novel eukaryotic vector. *Gene* 108: 193–199, 1991. doi: 10.1016/0378-1119(91)90434-D.

46. **Su J**, **Zhu Z**, **Xiong F**, **Wang Y**. Hybrid Cytomegalovirus-U6 Promoter-based Plasmid Vectors Improve Efficiency of RNA Interference in Zebrafish. *Mar Biotechnol* 10: 511–517, 2008. doi: 10.1007/s10126-008-9087-8.

47. **Moriya H**. Quantitative nature of overexpression experiments. *Mol Biol Cell* 26: 3932–3939, 2015. doi: 10.1091/mbc.E15-07-0512.

48. **Hamar J**, **Cnaani A**, **Kültz D**. Effects of CRISPR/Cas9 targeting of the myo-inositol biosynthesis pathway on hyper-osmotic tolerance of tilapia cells. *Genomics* 116: 110833, 2024. doi: 10.1016/j.ygeno.2024.110833.

49. **Concordet J-P**, **Haeussler M**. CRISPOR: intuitive guide selection for CRISPR/Cas9 genome editing experiments and screens. *Nucleic Acids Res* 46: W242–W245, 2018. doi: 10.1093/nar/gky354.

50. **Brinkman EK**, **Chen T**, **Amendola M**, **van Steensel B**. Easy quantitative assessment of genome editing by sequence trace decomposition. *Nucleic Acids Res* 42: e168, 2014. doi: 10.1093/nar/gku936.

51. **Bloh K**, **Kanchana R**, **Bialk P**, **Banas K**, **Zhang Z**, **Yoo B-C**, **Kmiec EB**. Deconvolution of Complex DNA Repair (DECODR): Establishing a Novel Deconvolution Algorithm for Comprehensive Analysis of CRISPR-Edited Sanger Sequencing Data. *CRISPR J* 4: 120–131, 2021. doi: 10.1089/crispr.2020.0022.

52. **Hamar J**, **Cnaani A**, **Kültz D**. Effects of CRISPR/Cas9 targeting of the myo-inositol biosynthesis pathway on hyper-osmotic tolerance of tilapia cells. *Genomics* Submitted, in review, [date unknown].

53. **Livak KJ**, **Schmittgen TD**. Analysis of Relative Gene Expression Data Using Real-Time Quantitative PCR and the 2−ΔΔCT Method. *Methods* 25: 402–408, 2001. doi: 10.1006/meth.2001.1262.

54. **Schmittgen TD**, **Livak KJ**. Analyzing real-time PCR data by the comparative CT method. *Nat Protoc* 3: 1101–1108, 2008. doi: 10.1038/nprot.2008.73.

55. **Cheung CY**, **Huang T-T**, **Chow N**, **Zhang S**, **Zhao Y**, **Chau MP**, **Chan WC**, **Wong CCL**, **Boassa D**, **Phan S**, **Ellisman MH**, **Yates JR**, **Xu S**, **Yu Z**, **Zhang Y**, **Zhang R**, **Ng LL**, **Ko BCB**. Unconventional tonicity-

regulated nuclear trafficking of NFAT5 mediated by KPNB1, XPOT and RUVBL2. *J Cell Sci* 135, 2022. doi: 10.1242/jcs.259280.

56. **Cheung CYK**, **Ko BCB**. NFAT5 in cellular adaptation to hypertonic stress – regulations and functional significance. *J Mol Signal* 8, 2013. doi: 10.1186/1750-2187-8-5.

57. **Kwon MS**, **Lim SW**, **Kwon HM**. Hypertonic Stress in the Kidney: A Necessary Evil. *Physiology* 24: 186–191, 2009. doi: 10.1152/physiol.00005.2009.

58. **Li J**, **Wang X**, **Lan T**, **Lu Y**, **Hong M**, **Ding L**, **Wang L**. CDK5/NFAT5-Regulated Transporters Involved in Osmoregulation in *Fejervarya cancrivora*. *Biology (Basel)* 11, 2022. doi: 10.3390/biology11060858.

59. **He M**, **Wei J**, **Li Y**, **Dong B**. Nuclear Factor of Activated T Cells-5 Regulates Notochord Lumenogenesis in Chordate Larval Development. *Int J Mol Sci* 23, 2022. doi: 10.3390/ijms232214407.

60. **Chernyakov D**, **Fischer A**, **Brandau M**, **Petrillo F**, **Fenton RA**, **Edemir B**. The nuclear factor of activated T cells 5 (NFAT5) contributes to the renal corticomedullary differences in gene expression. *Sci Rep* 12: 20304, 2022. doi: 10.1038/s41598-022-24237-y.

61. **Kok FO**, **Shin M**, **Ni C-W**, **Gupta A**, **Grosse AS**, **van Impel A**, **Kirchmaier BC**, **Peterson-Maduro J**, **Kourkoulis G**, **Male I**, **DeSantis DF**, **Sheppard-Tindell S**, **Ebarasi L**, **Betsholtz C**, **Schulte-Merker S**, **Wolfe SA**, **Lawson ND**. Reverse genetic screening reveals poor correlation between morpholino-induced and mutant phenotypes in zebrafish. *Dev Cell* 32: 97–108, 2015. doi: 10.1016/j.devcel.2014.11.018.

62. **Anrather J**, **Csizmadia V**, **Brostjan C**, **Soares MP**, **Bach FH**, **Winkler H**. Inhibition of bovine endothelial cell activation in vitro by regulated expression of a transdominant inhibitor of NF-kappa B. *J Clin Invest* 99: 763–772, 1997. doi: 10.1172/JCI119222.

63. **Macián F**, **García-Rodríguez C**, **Rao A**. Gene expression elicited by NFAT in the presence or absence of cooperative recruitment of Fos and Jun. *EMBO J* 19: 4783–4795, 2000. doi: 10.1093/emboj/19.17.4783.

64. **Takahashi K**, **Tanabe K**, **Ohnuki M**, **Narita M**, **Ichisaka T**, **Tomoda K**, **Yamanaka S**. Induction of Pluripotent Stem Cells from Adult Human Fibroblasts by Defined Factors. *Cell* 131: 861–872, 2007. doi: 10.1016/j.cell.2007.11.019.

65. **Baughman HER**, **Narang D**, **Chen W**, **Villagrán Suárez AC**, **Lee J**, **Bachochin MJ**, **Gunther TR**, **Wolynes PG**, **Komives EA**. An intrinsically disordered transcription activation domain increases the DNA binding affinity and reduces the specificity of NFκB p50/RelA. *J Biol Chem* 298: 102349, 2022. doi: 10.1016/j.jbc.2022.102349.

66. **Afek A**, **Schipper JL**, **Horton J**, **Gordân R**, **Lukatsky DB**. Protein−DNA binding in the absence of specific base-pair recognition. *Proc Natl Acad Sci U S A* 111: 17140–17145, 2014. doi: 10.1073/pnas.1410569111.

67. **Lin CY**, **Lovén J**, **Rahl PB**, **Paranal RM**, **Burge CB**, **Bradner JE**, **Lee TI**, **Young RA**. Transcriptional amplification in tumor cells with elevated c-Myc. *Cell* 151: 56–67, 2012. doi: 10.1016/j.cell.2012.08.026.

68. **Banks CAS**, **Lee ZT**, **Boanca G**, **Lakshminarasimhan M**, **Groppe BD**, **Wen Z**, **Hattem GL**, **Seidel CW**, **Florens L**, **Washburn MP**. Controlling for gene expression changes in transcription factor protein networks. *Mol Cell Proteomics* 13: 1510–1522, 2014. doi: 10.1074/mcp.M113.033902.

69. **Kimberland ML**, **Hou W**, **Alfonso-Pecchio A**, **Wilson S**, **Rao Y**, **Zhang S**, **Lu Q**. Strategies for controlling CRISPR/Cas9 off-target effects and biological variations in mammalian genome editing experiments. *J Biotech* 284: 91–101, 2018. doi: 10.1016/j.jbiotec.2018.08.007.

70. **Cai Q**, **Ferraris JD**, **Burg MB**. High NaCl increases TonEBP/OREBP mRNA and protein by stabilizing its mRNA. *Am J Physiol Renal Physiol* 289: F803-807, 2005. doi: 10.1152/ajprenal.00448.2004.

71. **Sacchi R**, **Gardell AM**, **Chang N**, **Kültz D**. Osmotic regulation and tissue localization of the *myo*-inositol biosynthesis pathway in tilapia (*Oreochromis mossambicus*) larvae. *J Exp Zool A Ecol Genet Physiol* 321: 457–466, 2014. doi: 10.1002/jez.1878.

72. **Lema SC**, **Carvalho PG**, **Egelston JN**, **Kelly JT**, **McCormick SD**. Dynamics of Gene Expression Responses for Ion Transport Proteins and Aquaporins in the Gill of a Euryhaline Pupfish during Freshwater and High-Salinity Acclimation. *Physiol Biochem Zool* 91: 1148–1171, 2018. doi: 10.1086/700432.

73. **Yamaguchi Y**, **Breves JP**, **Haws MC**, **Lerner DT**, **Grau EG**, **Seale AP**. Acute salinity tolerance and the control of two prolactins and their receptors in the Nile tilapia (*Oreochromis niloticus*) and Mozambique tilapia (*O. mossambicus*): A comparative study. *Gen Comp Endocrinol* 257: 168–176, 2018. doi: 10.1016/j.ygcen.2017.06.018.

74. **Esensten JH**, **Tsytsykova AV**, **Lopez-Rodriguez C**, **Ligeiro FA**, **Rao A**, **Goldfeld AE**. NFAT5 binds to the TNF promoter distinctly from NFATp, c, 3 and 4, and activates TNF transcription during hypertonic stress alone. *Nucleic Acids Res* 33: 3845–3854, 2005. doi: 10.1093/nar/gki701.

75. **Lopez-Rodríguez C**, **Aramburu J**, **Rakeman AS**, **Rao A**. NFAT5, a constitutively nuclear NFAT protein that does not cooperate with Fos and Jun. *Proc Natl Acad Sci U S A* 96: 7214–7219, 1999. doi: 10.1073/pnas.96.13.7214.

76. **Li S-Z**, **McDill BW**, **Kovach PA**, **Ding L**, **Go WY**, **Ho SN**, **Chen F**. Calcineurin-NFATc signaling pathway regulates AQP2 expression in response to calcium signals and osmotic stress. *Am J Physiol Cell Physiol* 292: C1606-1616, 2007. doi: 10.1152/ajpcell.00588.2005.

77. **Raat NJ**, **van Os CH**, **Bindels RJ**. Effects of osmotic perturbation on [Ca2+]i and pHi in rabbit proximal tubular cells in primary culture. *Am J Physiol* 269: F205-211, 1995. doi: 10.1152/ajprenal.1995.269.2.F205.

78. **Erickson GR**, **Alexopoulos LG**, **Guilak F**. Hyper-osmotic stress induces volume change and calcium transients in chondrocytes by transmembrane, phospholipid, and G-protein pathways. *J Biomech* 34: 1527–1535, 2001. doi: 10.1016/S0021-9290(01)00156-7.

79. **Apostol S**, **Ursu D**, **Lehmann-Horn F**, **Melzer W**. Local calcium signals induced by hyper-osmotic stress in mammalian skeletal muscle cells. *J Muscle Res Cell Motil* 30: 97–109, 2009. doi: 10.1007/s10974-009-9179-8.

80. **Ma A**, **Cui W**, **Wang X**, **Zhang W**, **Liu Z**, **Zhang J**, **Zhao T**. Osmoregulation by the myo-inositol biosynthesis pathway in turbot Scophthalmus maximus and its regulation by anabolite and c-Myc. *Comp Biochem Physiol A Mol Integr Physiol* 242: 110636, 2020. doi: 10.1016/j.cbpa.2019.110636.

81. **Fiol DF**, **Chan SY**, **Kültz D**. Regulation of osmotic stress transcription factor 1 (Ostf1) in tilapia(*Oreochromis mossambicus*) gill epithelium during salinity stress. *J Exp Biol* 209: 3257–3265, 2006. doi: 10.1242/jeb.02352.

82. **Wong MK-S**, **Ozaki H**, **Suzuki Y**, **Iwasaki W**, **Takei Y**. Discovery of osmotic sensitive transcription factors in fish intestine via a transcriptomic approach. *BMC Genom* 15: 1134, 2014. doi: 10.1186/1471-2164-15-1134.

83. **Herbelet S**, **De Vlieghere E**, **Gonçalves A**, **De Paepe B**, **Schmidt K**, **Nys E**, **Weynants L**, **Weis J**, **Van Peer G**, **Vandesompele J**, **Schmidt J**, **De Wever O**, **De Bleecker JL**. Localization and Expression of Nuclear Factor of Activated T-Cells 5 in Myoblasts Exposed to Pro-inflammatory Cytokines or Hyperosmolar Stress and in Biopsies from Myositis Patients. *Front Physiol* 9: 126, 2018. doi: 10.3389/fphys.2018.00126.

84. **Kumar R**, **DuMond JF**, **Khan SH**, **Thompson EB**, **He Y**, **Burg MB**, **Ferraris JD**. NFAT5, which protects against hypertonicity, is activated by that stress via structuring of its intrinsically disordered domain. *Proc Natl Acad Sci U S A* 117: 20292–20297, 2020. doi: 10.1073/pnas.1911680117.

FIGURE LEGENDS

Figure 1. Characterization of NFAT5 mRNA isoform abundance patterns and sequences in isosmotic (IO) and hyperosmotic (HO) conditions. A: Agarose gel electrophoresis of different RT-PCR amplified regions of the NFAT5 cds from both IO and HO treatments showing greater abundance in all amplicons for HO treatments. Multiple bands of similar intensity from amplicon 4 indicate the presence of two variants of exon 11. A notably weaker intensity of amplicon 2 relative to amplicon 1 indicates that exon 2 is missing from most transcripts. A yellow arrow depicts the expected band for each amplicon. B: NFAT5 mRNA abundance relative to β-actin reference gene in IO and HO conditions (two sample *t* test, $n = 6$, $^{***}P \leq 0.001$) displayed as box whisker plots in which the top and bottom boundaries represent the 1st and 3rd quartiles of the data, the median of each group is indicated by a solid horizontal bar, vertical lines represent highest and lowest data points excluding the outliers, the mean of each group is indicated by a dashed line, and individual data points are indicated by open circles except outliers which are solid black. C: Assembled sequence of HO induced *O. mossambicus* NFAT5 transcript (MW075269.1) aligned with the predicted *O. niloticus* NFAT5 sequence containing all possible exons (XM_005467029). MW075269.1 is missing exon 2 and a 65 bp section of exon 11. Location of primers used to generate amplicons 1-4 in 1A also included. D: Critical protein domains identified in mammalian NFAT5 mapped to the *O. mossambicus* MW075269.1 cds based on alignment of individual domain amino acid sequence to predicted MW075269.1 amino acid sequence. Designed primer locations for PCR amplification of truncated NFAT5 cds for use as dominant negative mutant in subsequent experiments are indicated in green.

Figure 2. Construction and validation of the IMPA1.1-EGFP reporter. A: vector map of the IMPA1.1-EGFP reporter showing the boundaries of the IMPA1.1 regulatory region from 1065 5' of the transcription

start site (TSS) to the endogenous start codon of exon 3 (*1386 bp omitted by the PCR reaction). B: Validation of IMPA1.1-EGFP reporter showing strongly increased fluorescence after 24 hour HO treatment relative to IO controls. C: Engineered EF1a(I-)2 promoter from endogenous O. mossambicus OmEF1a showing inclusion of 5' UTR within the first two exons but deletion of the first intron and modified Kozak sequence to generate NotI restriction. D: Functional validation of EF1a(I-)2 promoter expressing RFP showing strong fluorescence.

Figure 3. Interactions between different NFAT5 versions and the IMPA1.1 promoter. A: CMVIE-OmAP(I-)2 promoter engineered from endogenous *O. mossambicus* OmBact for NFAT5DN expression showing inclusion of 5' UTR within the first two exons but deletion of the first intron, modified Kozak sequence to generate NotI restriction site, and inclusion of the cytomegalovirus immediate early enhancer (CMVIE) at the 5' end. B&C: effect of different NFAT5 variants on relative fluorescence intensity (RFI) of the IMPA1.1 EGFP reporter displayed as box whisker plots as described in Figure 1. B: Suppression of HO induced RFI with increasing NFAT5DN (t test of regression slope , n = 4, **P ≤ 0.01). No data dispersion was observed in the IO condition as values of all replicates were measured to be close to zero. C: Induction of RFI by NFAT5WT in IO conditions (two sample t test, n = 2, **P ≤ 0.01). Mean and median values are overlapping in this data set.

Figure 4. Selection of target regions for development of NFAT5 KO cell lines. A: amino acid (aa) sequence alignment of predicted NFAT5 proteins from three fish species (*Oreochromis niloticus*, *Oryzias latipes*, and *Fundulus heteroclitus*) to identify highly conserved regions assumed to be essential sequence for gRNA targeting. The corresponding nucleotide sequence of the conserved (boxed) region was loaded into the CRISPOR gRNA selection algorithm. B: NFAT5 genomic locations corresponding to conserved aa sequence region and selected gRNAs from the CRISPOR output for *in vivo* empirical testing. Includes locations of the primer pairs used to generate test amplicons for mutational efficiency quantification and genotyping.

Figure 5. Genotype sequence output from DECODR algorithm analysis of test amplicon chromatograms from both initial screening process (Init.) and at the end of the experiment after multiple passages (post) on the selected clonal NFAT5 KO cell line for each gRNA (clone ID). For each INDEL (insertion/deletion mutation) the net bp change (INDEL ID), precise allele sequence at the targeted site relative to the wild-type sequence, the predicted relative frequency of each allele (Freq %), and the R2 model fit of each chromatogram input to the DECODR algorithm are shown.

Figure 6. Relative mRNA abundance of MIPS (A&B) and IMPA1.1 (C&D) genes quantified by qRT-PCR in NFAT5 KO cells lines compared to NE KO controls in both IO and HO conditions normalized using both β-actin and 18s rRNA as reference genes. Relative mRNA abundance of MIPS and IMPA1.1 transcripts are displayed as ($2^{-\Delta Ct}$)(53, 54) in box whisker plots as described in Figure 1. For all trials A-D, two sample *t* test, $n = 3$, $*P \leq 0.05$.

TABLES

			O. mossambicus NFAT5 cds Sequence Assembly	
Amplicon	Forward Primer ID	Reverse Primer ID	Forward Primer Sequence (5'-3')	Reverse Prim

1	NFAT5_F1	NFAT5X3_R1	ATGCCCTCTGACTTTATCTCCC	CTTCCTTTATGTCCTCC
2	NFAT5X2_F3	NFAT5X3_R1	GTCAAAAGAGCGGCGGAGA	CTTCCTTTATGTCCTCC
3	NFAT5X4_F1	NFAT5X8_R1	TCTGATGAACCTAGGACTACTAATC	GCTCCATGTCAATTTC
4	NFAT5X8_F1	NFAT5X12_R1	GGCTGAAATTGACATGGAGC	GCCCGCAACAATGTCC
5	NFAT5_F1	NFAT5X12_R1	ATGCCCTCTGACTTTATCTCCC	GCCCGCAACAATGTCC
6	NFAT5X12_F1	NFAT5X13_R1	AGACTGGTGATCTGCGTCCA	TTAGTAGGAACGAGT
7	NFAT5X7_F3	NFAT5X12(XbaI)_R1	CCCCCAAGCTTGGTCTCAGAGGAGGTCTTCATC	CCCCCTCTAGAGCCCG
8	NFAT5X12_F1b	NFAT5X12_R4	CCCCCCTCGAGAGACTGGTGATCTGCGTCCA	TGTTGAGGCTGAGATC
9	NFAT5X12_F7b	NFAT5X13_R2b	CCCCCCTCGAGATTTCAGACCCAGATCTCCC	CCCCCCTCAGATTAGT

O. mossambicus NFAT5 mRNA quantitative RT-PCR

Target Gene	Accession Number	Dilution	Forward Primer Sequence (5'-3')	Reverse Prim
NFAT5	NC031965	1:10	GAAGATCCTCGTCCAGCCTG	GCCAACGAACACCTGC
β-actin	AB037865	1:10	CCACAGCCGAGAGGGAAAT	CCCATCTCCTGCTCGA
18s Rrna	AF497908	1:10	CGATGCTCTTAGCTGAGTGT	ACGACGGTATCTGATC

Table 1. Primer pair sequence information associated with; RT-PCR generated amplicons used in sequencing and cloning of the HO induced *O. mossambicus* NFAT5 cds (MW075269.1), and qRT-PCR quantification of NFAT5 mRNA in IO and HO conditions.

Target #	gRNA Sequence	Test Amplicon (Primers and Length)			MIT Spec. Score	Doe Effici
		Forward Primer	Reverse Primer	Size (bp)		
T1	GTGAAGGACCGCACTCAGC	GCTGCAGCTCTGATGAACCT	CCTTAGAGCTTTGGTCCCCG	722	95	
T2	GGAAAGCCCTGCTGAGTG	GCTGCAGCTCTGATGAACCT	CCTTAGAGCTTTGGTCCCCG	722	92	
T3	GTTGCGACCAGTAACCCTGC	CAGCAGATCTACCAGGAGCG	CCTTGCTGGGTAATTTTCTGCA	667	94	
T4	GCAACACCACAGCCTGCA	CAGCAGATCTACCAGGAGCG	CCTTGCTGGGTAATTTTCTGCA	667	90	
T5	GCAAGGAGGTTGATATTGA	CAGCAGATCTACCAGGAGCG	CCTTGCTGGGTAATTTTCTGCA	667	92	
T6	GCTCCGCAACGCTGATGTAG	TCCAAGCTCCAACATGACCC	GCCCTAAGCGTCTTTCCTGT	738	97	
T7	GATGTAGAGGCTCGCATTG	TCCAAGCTCCAACATGACCC	GCCCTAAGCGTCTTTCCTGT	738	98	
T8	GACTGAACCATCTGGACG	TCCAAGCTCCAACATGACCC	GCCCTAAGCGTCTTTCCTGT	738	95	

Table 2. Candidate gRNA sequences selected for *in vivo* empirical testing of mutational efficiency including test amplicon sizes with associated primer pairs, CRISPOR MIT specificity scores, predicted efficiency (Doench) and *in vivo* empirically tested efficiency (TIDE INDEL%).


A
Amplicon 1
Exon 1 to Exon 3
Amplicon 2
Exon 2 to Exon 3
Amplicon 3
Exon 4 to Exon 8
Amplicon 4
Exon 8 to Exon 12
IO
HO
IO
HO
IO
HO
IO
HO
1000 bp
700 bp
500 bp

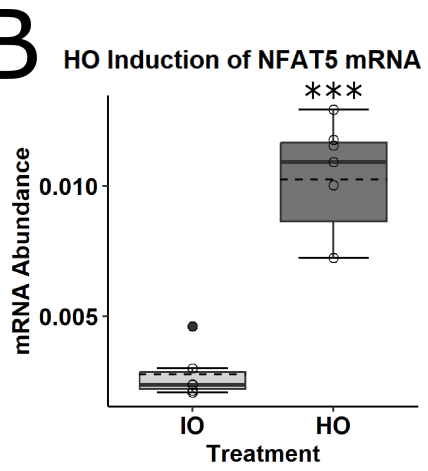
B
HO Induction of NFAT5 mRNA
***
mRNA Abundance
0.010
0.005
IO
HO
Treatment

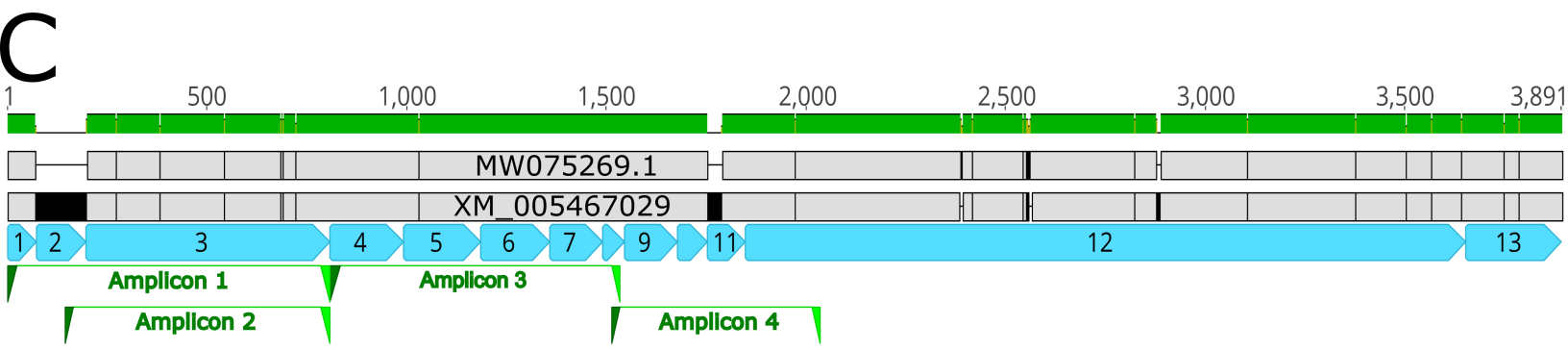
C
1
500
1,000
1,500
2,000
2,500
3,000
3,500
3,891
MW075269.1
XM_005467029
1
2
3
4
5
6
7
9
11
12
13
Amplicon 1
Amplicon 3
Amplicon 2
Amplicon 4

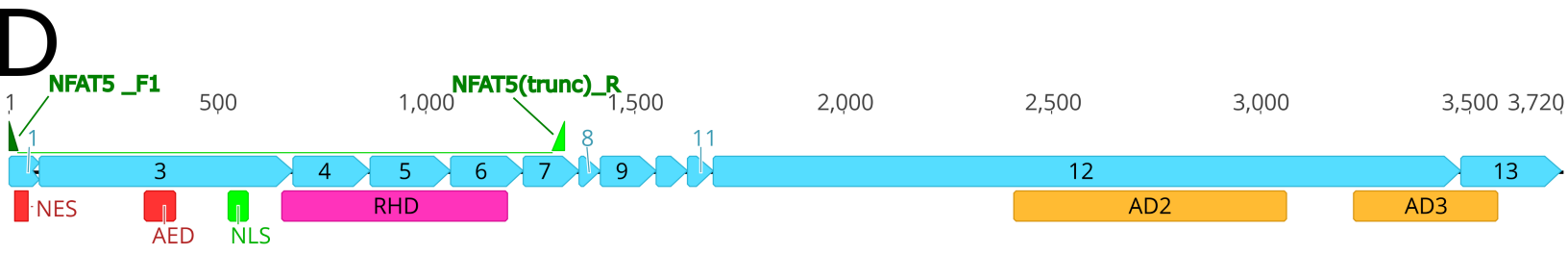
D
NFAT5 _F1
NFAT5(trunc)_R
1
500
1,000
1,500
2,000
2,500
3,000
3,500
3,720
1
8
11
3
4
5
6
7
9
12
13
NES
AED
NLS
RHD
AD2
AD3

A

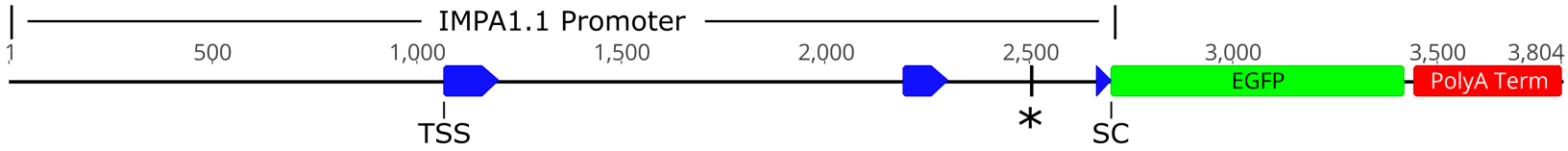
IMPA1.1 Promoter
1
500
1,000
1,500
2,000
2,500
3,000
3,500
3,804
EGFP
PolyA Term
TSS
SC

B

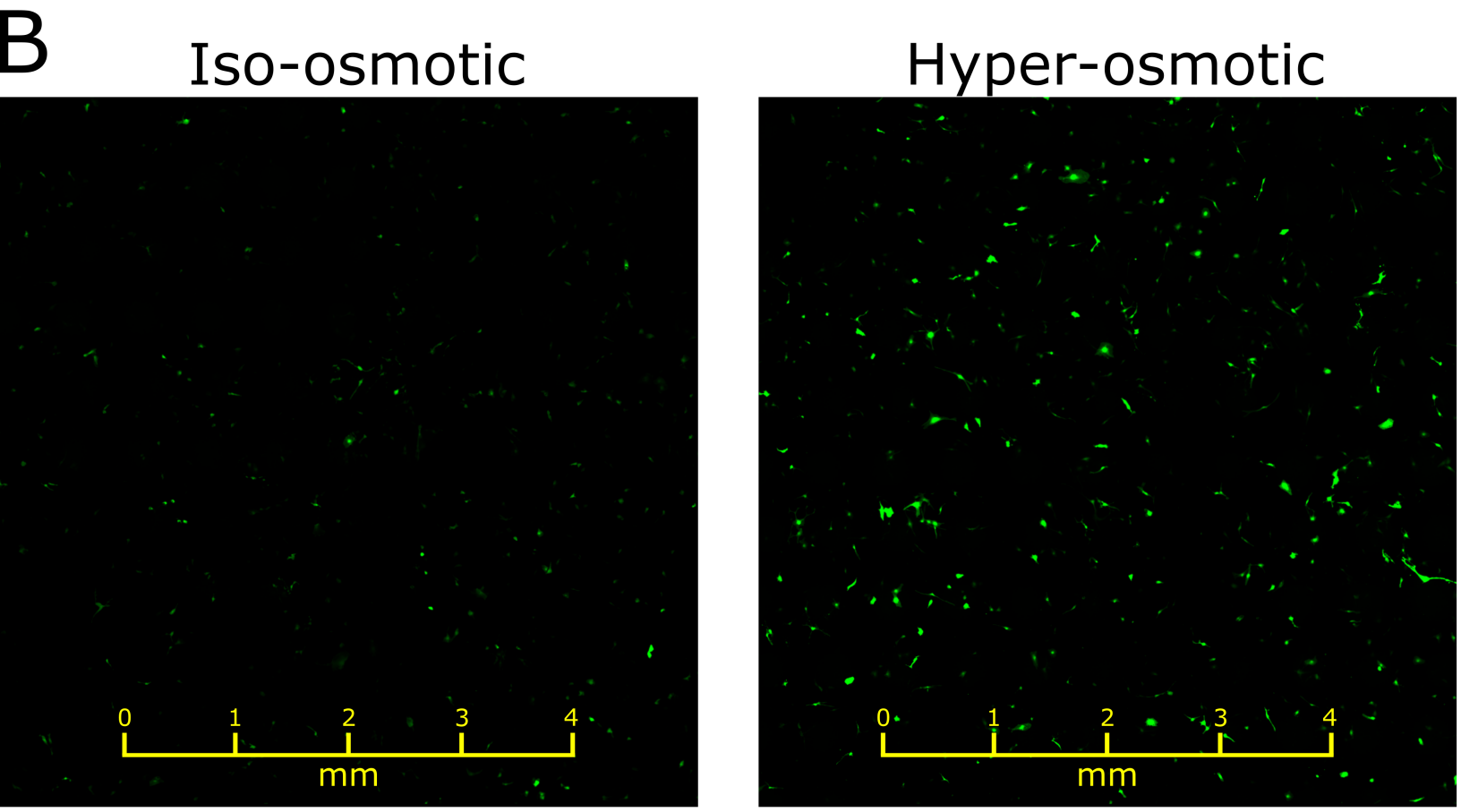
Iso-osmotic
Hyper-osmotic
0
1
2
3
4
mm

C

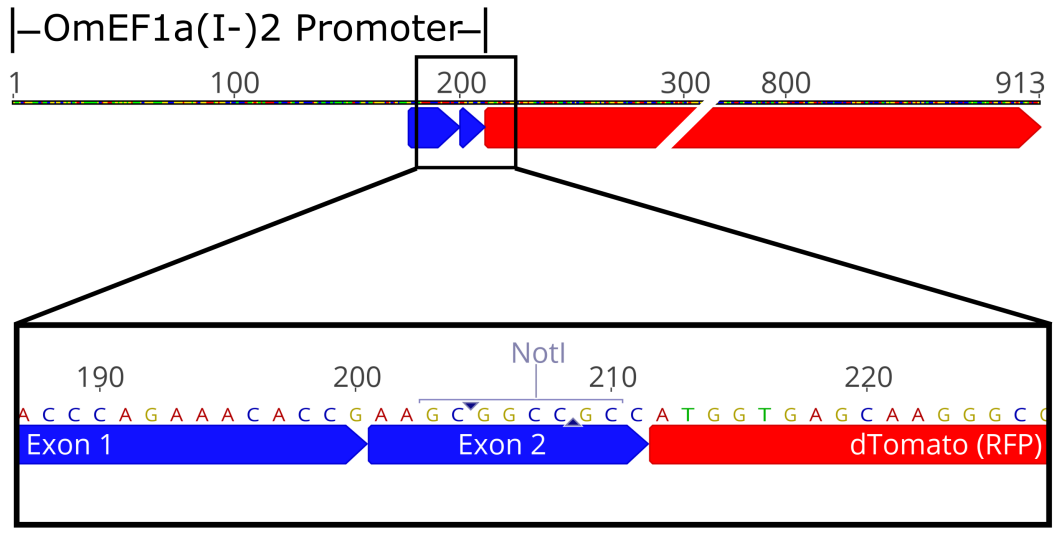
OmEF1a(I-)2 Promoter
1
100
200
300
800
913
NotI
190
200
210
220
Exon 1
Exon 2
dTomato (RFP)

D

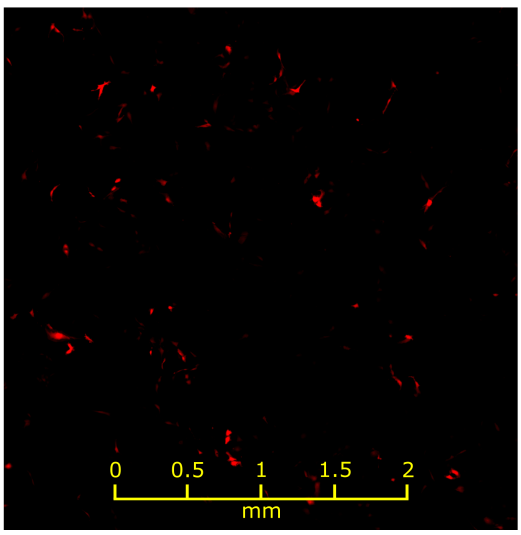
0
0.5
1
1.5
2
mm

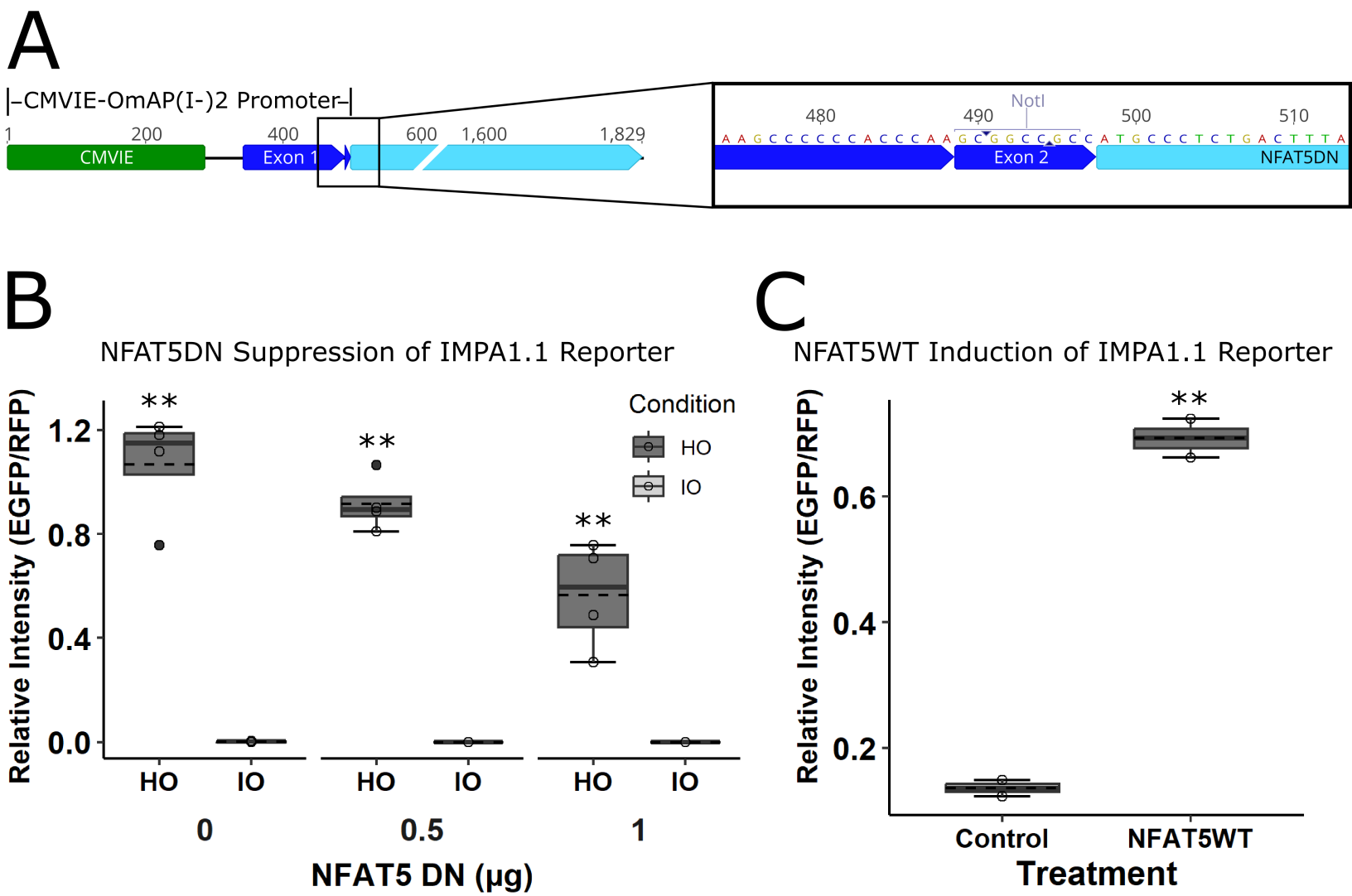
A
|–CMVIE-OmAP(I-)2 Promoter–|
1
200
400
600
1,600
1,829
CMVIE
Exon 1
480
490
500
510
NotI
Exon 2
NFAT5DN
B
NFAT5DN Suppression of IMPA1.1 Reporter
Relative Intensity (EGFP/RFP)
1.2
0.8
0.4
0.0
**
Condition
HO
IO
HO
IO
0
0.5
1
NFAT5 DN (µg)
C
NFAT5WT Induction of IMPA1.1 Reporter
Relative Intensity (EGFP/RFP)
0.6
0.4
0.2
**
Control
NFAT5WT
Treatment

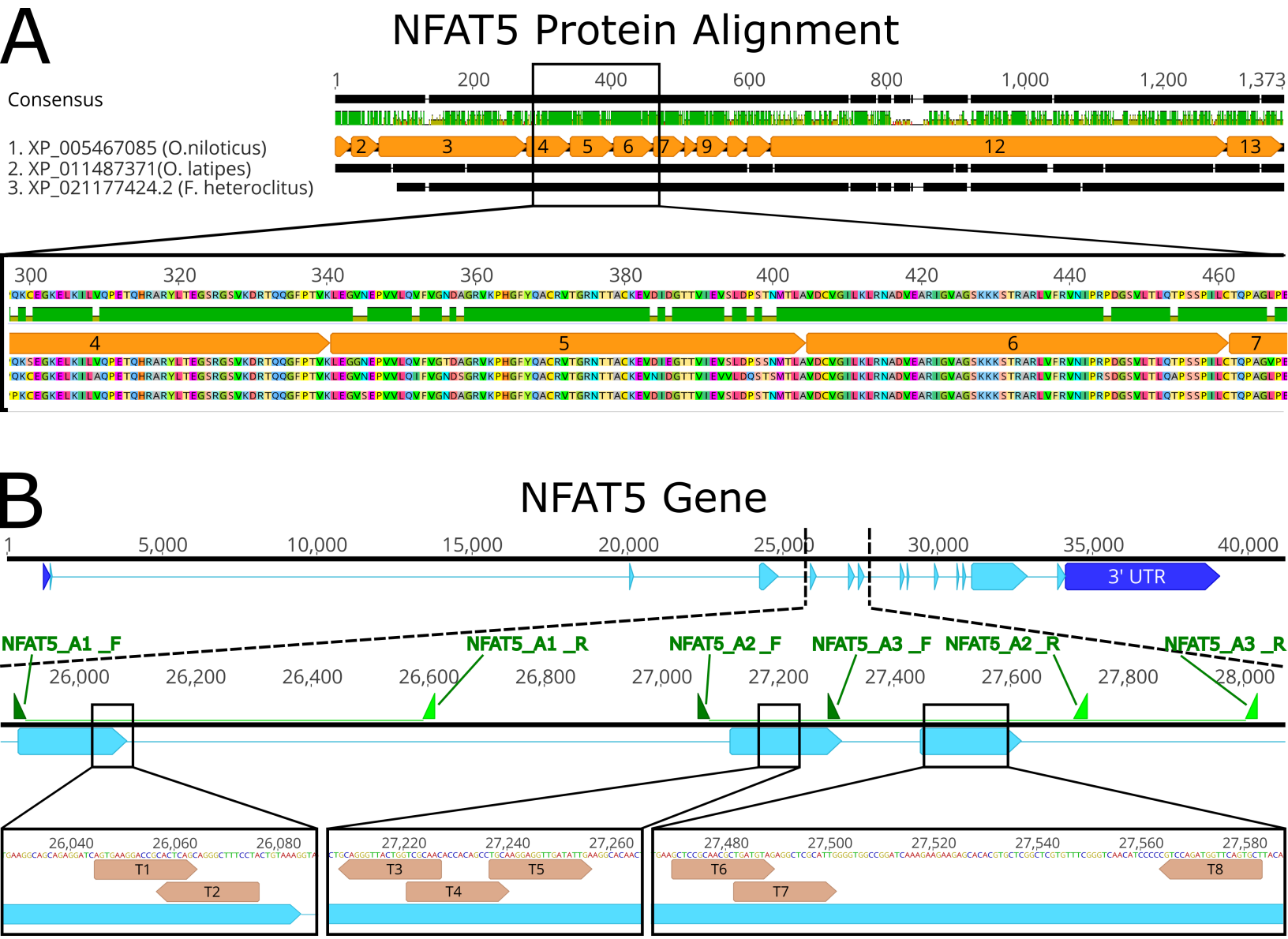
A
NFAT5 Protein Alignment
Consensus
1. XP_005467085 (O.niloticus)
2. XP_011487371(O. latipes)
3. XP_021177424.2 (F. heteroclitus)
1
200
400
600
800
1,000
1,200
1,373
2
3
4
5
6
7
9
12
13
300
320
340
360
380
400
420
440
460

B
NFAT5 Gene
1
5,000
10,000
15,000
20,000
25,000
30,000
35,000
40,000
3' UTR
NFAT5_A1 _F
NFAT5_A1 _R
NFAT5_A2 _F
NFAT5_A3 _F
NFAT5_A2 _R
NFAT5_A3 _R
26,000
26,200
26,400
26,600
26,800
27,000
27,200
27,400
27,600
27,800
28,000
26,040
26,060
26,080
T1
T2
27,220
27,240
27,260
T3
T4
T5
27,480
27,500
27,520
27,540
27,560
27,580
T6
T7
T8

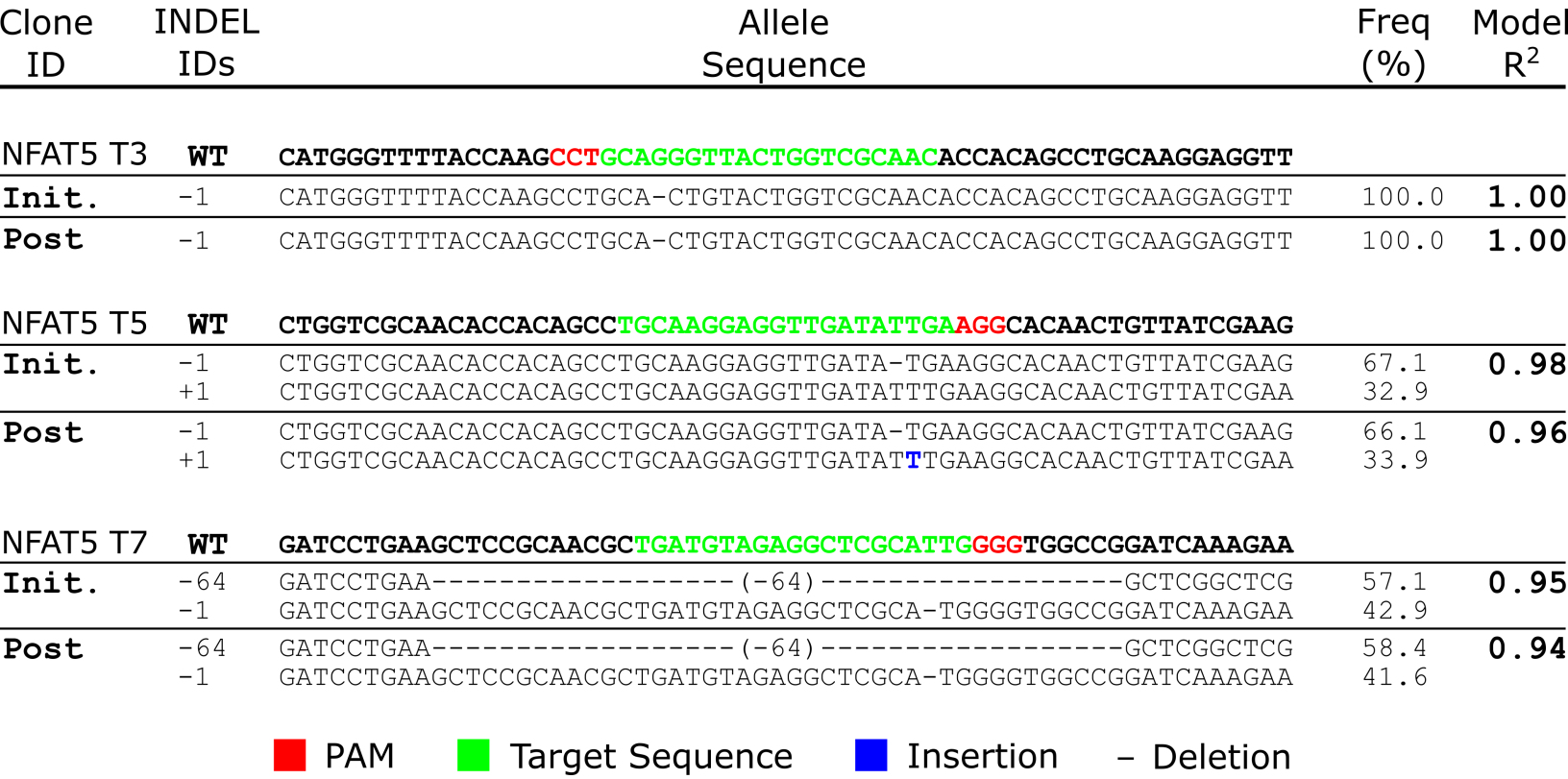
Clone ID
INDEL IDs
Allele Sequence
Freq (%)
Model R^2
NFAT5 T3
WT CATGGGTTTTACCAAGCCTGCAGGGTTACTGGTCGCAACACCACAGCCTGCAAGGAGGTT
Init. -1 CATGGGTTTTACCAAGCCTGCA-CTGTACTGGTCGCAACACCACAGCCTGCAAGGAGGTT 100.0 1.00
Post -1 CATGGGTTTTACCAAGCCTGCA-CTGTACTGGTCGCAACACCACAGCCTGCAAGGAGGTT 100.0 1.00
NFAT5 T5
WT CTGGTCGCAACACCACAGCCTGCAAGGAGGTTGATATTGAAGGCACAACTGTTATCGAAG
Init. -1 CTGGTCGCAACACCACAGCCTGCAAGGAGGTTGATA-TGAAGGCACAACTGTTATCGAAG 67.1 0.98
+1 CTGGTCGCAACACCACAGCCTGCAAGGAGGTTGATATTTGAAGGCACAACTGTTATCGAA 32.9
Post -1 CTGGTCGCAACACCACAGCCTGCAAGGAGGTTGATA-TGAAGGCACAACTGTTATCGAAG 66.1 0.96
+1 CTGGTCGCAACACCACAGCCTGCAAGGAGGTTGATATTTGAAGGCACAACTGTTATCGAA 33.9
NFAT5 T7
WT GATCCTGAAGCTCCGCAACGCTGATGTAGAGGCTCGCATTGGGGTGGCCGGATCAAAGAA
Init. -64 GATCCTGAA----------(-64)----------GCTCGGCTCG 57.1 0.95
-1 GATCCTGAAGCTCCGCAACGCTGATGTAGAGGCTCGCA-TGGGGTGGCCGGATCAAAGAA 42.9
Post -64 GATCCTGAA----------(-64)----------GCTCGGCTCG 58.4 0.94
-1 GATCCTGAAGCTCCGCAACGCTGATGTAGAGGCTCGCA-TGGGGTGGCCGGATCAAAGAA 41.6
PAM
Target Sequence
Insertion
– Deletion

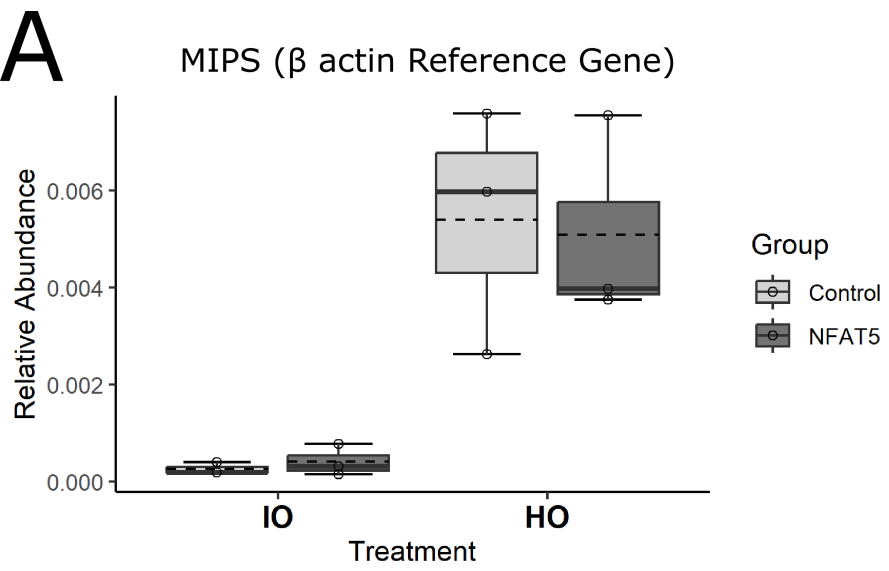
A
MIPS (β actin Reference Gene)
Relative Abundance
0.006
0.004
0.002
0.000
IO
HO
Treatment
Group
Control
NFAT5

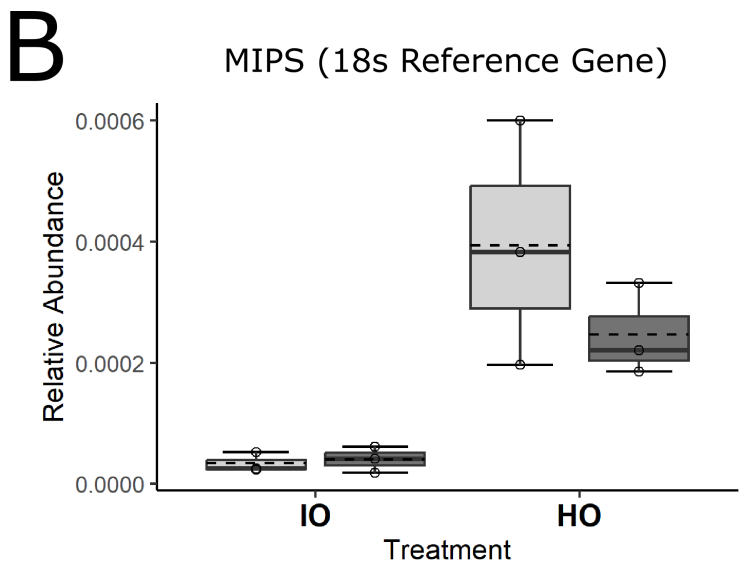
B
MIPS (18s Reference Gene)
Relative Abundance
0.0006
0.0004
0.0002
0.0000
IO
HO
Treatment

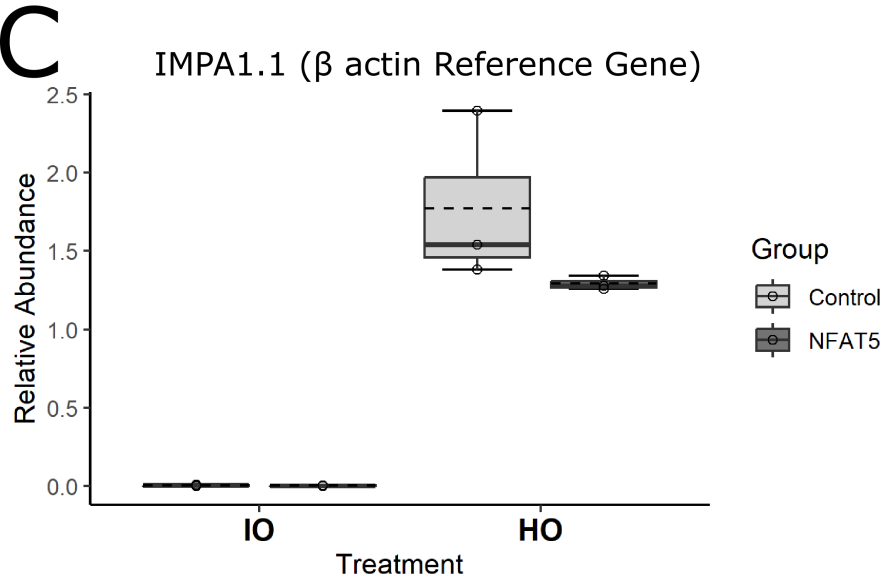
C
IMPA1.1 (β actin Reference Gene)
Relative Abundance
2.5
2.0
1.5
1.0
0.5
0.0
IO
HO
Treatment
Group
Control
NFAT5

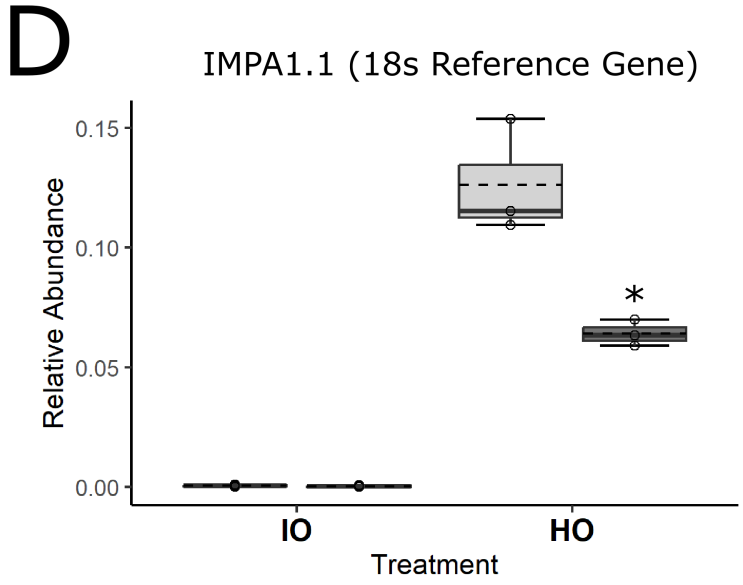
D
IMPA1.1 (18s Reference Gene)
Relative Abundance
0.15
0.10
0.05
0.00
*
IO
HO
Treatment

Osmotic regulation of myo-inositol biosynthesis (MIB) by NFAT5

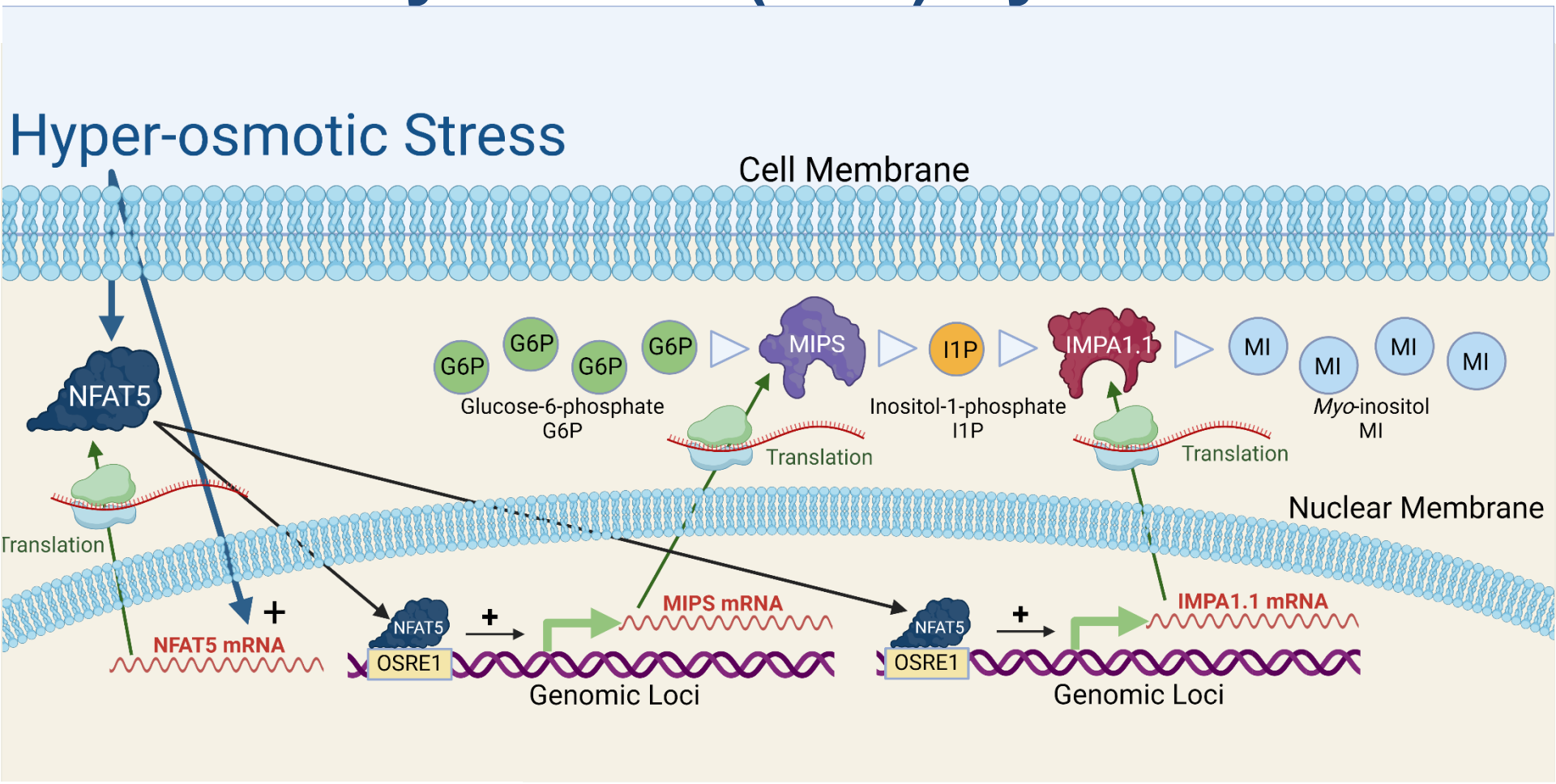

Overexpression of wild-type NFAT5 activates while dominant negative and CRISPR/Cas9 targeting of NFAT5 suppress activation of MIB promoters identifying NFAT5 as a primary MIB regulator in osmotically stressed tilapia cells.